ACROPOLIS
European NoE on Cognitive Communications

SEVENTH FRAMEWORK PROGRAMME

Advanced coexistence technologies for radio optimisation in licensed and unlicensed spectrum

(ACROPOLIS)

Document Number D13.1

Adaptive and robust signal processing algorithms for directive mapping in interference networks

Contractual date of delivery to the CEC:	31/03/2012
Actual date of delivery to the CEC:	31/03/2012
Project Number and Acronym:	257626 - ACROPOLIS
Editor:	Jing Lv (TUD), Eduard Jorswieck (TUD)
Authors:	Luca De Nardis (Uniroma1), Maria-Gabriella Di Benedetto (Uniroma1), Guido Carlo Ferrante (Uniroma1), Jing Lv (TUD), Eduard Jorswieck (TUD), Ragnar Thobaben (KTH), Valentin Rakovic (UKIM), Vladimir Atanasovski (UKIM), Liljana Gavrilovska (UKIM), Olasunkanmi Durowju (UoS), Kamran Arshad (UoS), Klaus Moessner (UoS)
Participants:	Uniroma1, TUD, KTH, UKIM, UoS
Workpackage:	WP13
Security:	Public (PU)
Nature:	Report
Version:	1.0
Total Number of Pages:	57

Abstract:

This deliverable describes a collection of signal processing and resource allocation algorithms under different reference scenarios in cognitive radio based on directives, decisions and constraints from the decision engine. Either the operation of the decision engine and the execution engine is decoupled by constraints and requirements formulated by the decision engine in terms of interference temperature constraints, guard bands, or spectral masks, or the decision and execution tasks are optimized jointly. In the first case, the decisions can be made without considering a certain hardware platform or transmission technique of the cognitive system. The task of the execution engine is then to map the constraints to the specific platform and to the available transmission techniques. In the second case, a close cooperation between both engines is required and the complexity as well as performance is increased.

Firstly, the most relevant models of coexistence of cognitive radio systems and legitimate systems are introduced, including interweave cognitive radio systems, underlay cognitive radio systems, and overlay cognitive radio systems, with the most relevant transceiver techniques in specific scenarios. For interweave cognitive radio, factors affecting the spectrum sensing reliability are introduced, including real-time operation and robustness to channel variations, and primary user protection mechanisms and rules are explained. For underlay cognitive radio, the interference constraint of the primary users can be met by using multiple antennas to guide the secondary signals away from the primary receivers, or UWB technique, where coding shaping and pulse shaping are illustrated for spectrum shaping in Impulse-Radio-based UWB, and coexistence requirements and capabilities of OFDM-based UWB systems were investigated. For overlay cognitive radio, cooperation strategy between the primary and secondary system on the transmitter side or the receiver side is introduced.

Then, decision parameters and the influence of the execution algorithm on the physical layer are described, including the constraints and requirements formulated by the decision engine, which define the interface between decision and execution. For the network layer, end-to-end delay/throughput, mobility management and traffic classes are introduced and how they are mapped to the physical layer are described. For the MAC layer, rate/delay requirements, queuing and stability are introduced and how they are mapped to the physical layer are described. For the physical layer, spectrum sensing, channel coding and decoding, rate splitting and successive decoding, and channel state information acquisition are introduced and how they are mapped to the hardware parameters are described.

At last, several signal processing and resource allocation algorithms are explained, including optimal beamforming in MISO cognitive channels with noncausal primary message, distributed power control for cognitive radios with primary protection via spectrum sensing, precoding of UWB signals by Time Reversal. The performance of algorithms is evaluated through simulation, and implementation complexity and feedback/control requirements are analysed.

Keywords: Decision parameters, directives mapping, signal processing and resource allocation

Document Revision History

Version	Date	Author	Summary of main changes
0.1	04.02.2011	TUD	Initial structure of the document
0.2	08.03.2011	TUD	Revised structure according to discussions during the Cluster 3 meeting in Aachen on Feb. 17, 2011
0.3	13.04.2011	TUD	Added explanation in introduction according to WP13 telco. Added bullet points for discussion in D13.1 telco (14.04.2011).
0.4	15.09.2011	TUD	Added comments/contributions bullet points from KTH and TUD for discussion in D13.1 telco (15.09.2001).
0.5	24.10.2011	TUD	Added bullet points from UKIM, UoS and Uniroma1
0.6	25.10.2011	TUD	Added bullet points
0.7	06.11.2011	TUD	Added draft text input
0.71	18.11.2011	UKIM	Added draft text input
0.72	21.11.2011	KTH	Added draft text input
0.73	29.11.2011	UoS	Added draft text input
0.74	10.12.2011	Uniroma1	Added draft text input
0.8	20.02.2012	TUD	Editing
0.9	28.02.2012	TUD	Update after the ACROPOLIS meeting in Ispra
0.91	14.03.2012	TUD	Update based on the comments from partners
0.92	19.03.2012	TUD	Revision after submission to ACROPOLIS Executive Committee
0.93	19.03.2012	TUD	Revision
1.0	29.03.2012	TUD	Revision, final version

Table of Contents

1. Introduction

WP13 implements the directives and decisions from the decision engine on all relevant layers of the protocol stack, from network layer, MAC, to the PHY layer. Since different hardware platforms are addressed, the directives need to be mapped to hardware parameters and concrete physical parameters of the radio frontend. WP13 is the interface between the execution engine and the real implementation on a specific hardware platform.

The traditional approach to analyse and design complex communications systems is layering and modelling of a small part of the system in an idealized way. In a cognitive radio system, the most challenging and important impact is created by interference on the physical layer. Therefore, a careful modelling of the interference created in different operation modes of cognitive radio systems is required. Based on the interference model and a set of carefully selected system parameters, the achievable performance is characterized. The achievable performance is then used as input to the decision engine.

A dependency cycle between the decision engine and the execution task is identified. Obviously, the execution depends on the orders and instructions of the decision engine. Furthermore, the parametric model of the executed communication scenario is required by the decision engine to decide on the operation mode and resource allocation. There are two possibilities to resolve the cyclic dependency: Either the modelling and parameterization task is separated from the decision by defining static execution strategies and a clear interface, or an iterative joint optimization process is developed. It depends on the complexity and constraints which method is preferred. In both cases a certain operating point is required either for an initial staring point or for a static execution strategy.

The interface between decision engine and execution engine is briefly described and the relationship to the deliverable structure is discussed in the following. The execution engine works on different cognitive radio system scenarios (interweave, overlay, and underlay). Each scenario is described by a set of parameters and constraints. The scenarios and their parameters are discussed in Section 2. The mapping from decision engine directives to execution can be understood as an order, which consists of a choice of the scenario and an instantiation of the corresponding parameter set. The parameter sets which are used to define the directives are proposed and studied in Section 3. Finally, the achieved performance for instantiated parameter sets needs to be computed and should be available to the decision engine. In Section 4, for each scenario one representative example is provided in order to understand how the transceiver structure influences the choice of the parameter sets and the achievable performance. Section 5 concludes the deliverable.

2. Cognitive Radio Paradigms and Concepts

In the following, the most relevant models of coexistence of cognitive radio systems and legitimate systems are introduced.

2.1 Interweave Cognitive Radio Systems

An interweave cognitive radio is an intelligent wireless communication system that periodically monitors the radio spectrum, intelligently detects occupancy in the different parts of the spectrum, and then opportunistically communicates over spectrum holes with minimal interference to the active user. Cognitive user transmits simultaneously with a non-cognitive user only in the event of a false spectral hole detection. Cognitive user's transmit power is limited by the range of its spectral hole sensing.

In the case of interweave Cognitive Radio (CR) systems, Secondary Users (SUs) utilize vacant Primary Users (PUs) spectrum for their own communication purposes. This accentuates the necessity of reliable detection of the available spectrum currently not utilized by any PU. Inaccurate detection can result in excessive interference to the PU systems and can severely affect their performance. A possible method for vacant spectrum (i.e. PU absence) detection is spectrum sensing that utilizes techniques which strongly rely on signal processing. There are several spectrum sensing techniques [1], which differ according to the amount of needed a priori information for proper operation, implementation complexity, accuracy etc.

There are numerous factors affecting the spectrum sensing reliability. The most essential ones are real-time operation and robustness to channel variations depending on the device performance and the channel state. The sensing period and the computational complexity have a strong influence on the real-time sensing capabilities, e.g. long sensing periods or methods with higher computational complexity increase the detection performance, but decrease the real-time operation. The robustness to channel variations is mainly influenced by the impact of the noise and the fading, which may affect the reliability and the performance of the spectrum sensing techniques. Many solutions propose to mitigate the negative noise and fading effects by introducing complex signal processing techniques as well as cooperation between multiple sensing devices.

As already elaborated, real-time operation is a vital reliability factor of any spectrum sensing technique which is tightly correlated with its detection performance. For example, in the case of AWGN channel, the detection performance of the conventional energy based detector [1][2], which uses only the power of the received samples, increases when the number of sensed samples increases

$$P_d = Q_{N/2}(\sqrt{N\gamma}, \sqrt{\lambda/2}) \quad (2.1.1)$$

$$P_f = \frac{\Gamma(N/2, \lambda/2)}{\Gamma(N/2)} \quad (2.1.2)$$

where P_d, P_f, N, γ and λ represent the probability of detection, probability of false alarm, number of sensed samples, channel SNR and SNR threshold, respectively, while $Q_{N/2}(\cdot,\cdot)$,

$\Gamma(\cdot)$ and $\Gamma(\cdot,\cdot)$ denote the generalized Marcum Q-function, Gamma and incomplete Gamma functions, respectively. Equation (2.1.2) shows that higher number of sensed samples can be obtained either when increasing the sensing time or the sampling frequency of the device

$$N = T_s f_s \tag{2.1.3}$$

where f_s and T_s, denote the sampling frequency and the sensing time, respectively. Hence, the spectrum sensing techniques cannot use very long sensing periods in order to stay in the boundaries of real-time operation. The same conclusions, about the real-time operation, can be made for all types of energy based detectors (e.g. eigen value detector, Higher Order Statistics - HOS detector etc.).

In the case of feature detection techniques, the real-time operation reliability factor is also related to the sensing time and the computational complexity. Longer observation times usually result in higher reliability since the feature based sensing techniques exploit the correlation properties of the PU signal type. However, [3] proves that the length of the sensing time of a cyclostationarity based detector, needed for reliable PU detection, is significantly small and satisfies the real-time requirements. On the other hand, the computational complexity can have a significant impact on the real-time performance of feature based spectrum sensing techniques. Due to the complex mathematical operations, these spectrum sensing techniques require devices with high processing power. Compared to the energy based, feature based techniques prove to struggle more in terms of the real-time reliability factor.

In the concept of cooperative spectrum sensing [1], the bottleneck of the real-time reliability is due to the small bandwidth of the control (reporting) channel. Large number of cooperative nodes can easily congest the control channel and increase the reporting time, thus decrease the real-time reliability of the sensing technique. For example, if the bandwidth of the control channel is *B* and the number of users is *N* then the reporting time τ_R will be defined as

$$\tau_R = \sum_{i=1}^{N} \frac{1}{B} = \frac{N}{B} \tag{2.1.4}$$

It is evident from (2.1.4) that higher number of cooperating nodes can substantially increase the reporting time especially if the control channel bandwidth is small (which is usually the case in cooperative spectrum sensing).

As previously mentioned, another essential reliability factor of the spectrum sensing techniques is the robustness to channel variations in terms of noise and fading. It is proven that in noisy environments the conventional energy detection underperforms due to the noise uncertainty [1]. In this case, if the noise level is not precisely known, the detection becomes impossible for low signal levels. More sophisticated energy based detection techniques (e.g. eigen value detector, HOS detector etc.), feature based detectors, as well as cooperative spectrum sensing techniques overcome the noise uncertainty problem and provide reliable performance in cases of highly noised channels. For instance, the detection performance (probability of detection and probability of false alarm) of an energy based cooperative spectrum sensing technique that utilizes the Equal Gain Combining (EGC) fusion rule [2] are given with

$$P_d = Q_{KN/2}(\sqrt{KN\gamma}, \sqrt{\lambda/2}) \quad (2.1.5)$$

$$P_f = \frac{\Gamma(KN/2, \lambda/2)}{\Gamma(KN/2)} \quad (2.1.6)$$

where *K* denotes the number of users, while the other parameters are the same as the ones previously defined in equations (2.1.1) and (2.1.2). When comparing equations (2.1.1) with (2.1.5) and (2.1.2) with (2.1.6), it is evident that the noise uncertainty problem diminishes if the number of cooperating nodes is sufficiently high.

Another parameter that can have severe impact on the reliability of the spectrum sensing techniques is the channel fading. When a single node is used for spectrum sensing, fading environments can substantially decrease the spectrum sensing reliability regardless of the spectrum sensing technique. The cooperation among nodes in a cognitive radio network i.e. cooperative spectrum sensing can help overcome the fading drawback since it introduces a form of spatial diversity that results in collaboration gain [1]. Correlated shadowing is another feature that can affect the spectrum sensing reliability especially when considering cooperative spectrum sensing. The correlation between the sensed data of spatially distributed nodes is dependent on the distance among the nodes. In correlated environments (e.g. log-normal shadowing), the nodes should be physically separated on a distance that provides the satisfactory gain. However, they should be also close enough in order to actually cooperate. Therefore, node selection is a vital process that enhances the performance of cooperative spectrum sensing in correlated shadowing environments, but can significantly increase the system and deployment complexity.

There are many incumbent primary communication systems (e.g. DTV, radar, DME etc.) which implement sparse frequency planning with large interference margins. This leads to an underutilization of frequency spectrum in a given geographic area and an SU operating on a vacant frequency spectrum chunk at relatively low power level would not need a great separation from co-channel and adjacent channel PUs to avoid causing interference. This opportunistic operation of SUs in the interleaved spectrum holes is conditioned on their ability to avoid harmful interference to licensed PUs of these bands. Therefore, the SUs must be aware of the geographical and frequency characteristics of the primary system within the area of current location. However, the SUs must also incorporate certain regulatory rules which govern the particular frequency band and geographical location.

For example, the FCC rules [4][5][6] define a fixed permitted maximum transmit power for different types of TV white space devices. The maximum Equivalent Isotropicaly Radiated Power (EIRP) for a fixed TV white space device with an antenna height below 30 m is 39 dBm. For a mobile device, the EIRP limit is 20 dBm. There is an additional protection distance in which white space devices are not allowed to operate at all on the same channel around each TV transmitter coverage area. Outside this area, the permitted transmit power immediately goes up to the maximum allowed value. The FCC rules also forbid white space device usage in the first adjacent channel to an occupied DTV channel, but in this case the protection distance is smaller. For a white space device with antenna height between 10 m and 30 m, the added co-channel protection zone is 14.4 km and the adjacent channel

protection zone is 0.74 km. Beyond the first adjacent channel there are no limitations from the viewpoint of one particular transmitter.

On the other hand, the ECC rules [7] allowed SUs to transmit at different power levels based on their distance to the coverage area. The protection principle is implemented as a boundary condition of the maximum transmission power. The method developed by SE43 calculates the permitted maximum transmit power for a white space device at a given location. The calculation lays on the given permitted degradation of location probability for TV reception. Furthermore, the ECC has left specification of white space device spectrum masks to manufactures, while FCC has prescribed stringent masks.

2.2 Underlay Cognitive Radio Systems

The underlay paradigm mandates that concurrent noncognitive and cognitive transmissions may occur only if the interference generated by the cognitive devices at the noncognitive receivers is below some acceptable threshold. The interference constraint for the noncognitive users may be met by using multiple antennas to guide the cognitive signals away from the noncognitive receivers, or by using a wide bandwidth over which the cognitive signal can be spreaded below the noise floor, then despreaded at the cognitive receiver.

In general, for underlay CR settings the degradation in terms of quality of service (QoS) to the primary user is a critical aspect. In [8] interference temperature constraints (ITC) [9] were used to measure and limit this effect. In a multiple antenna system, the ITCs are distinguished in soft- and peak power-shaping constraints [10]. These constraints refer to the maximum average power and average peak power tolerated at the primary receivers, respectively. [11] considers the setting of a single secondary user sharing the same spectral band with multiple primary users. The authors provide optimal transmit beamforming strategies under ITCs for the secondary user. Furthermore, [12] characterizes the Pareto boundary of the multiple-input single-output (MISO) interference channel (IFC) through controlling the ITCs at the receivers. Convex optimization techniques for solving CR problems are studied in [13]. The coexistence of a single-input single-output (SISO) primary link and a MISO secondary link is considered in [14], where the achievable secondary rate is optimized under the primary rate constraint, assuming the primary link does not fully load its rate to achieve the Shannon capacity with equality, but there is room that can be exploited by spatial shaping (beamforming) at the secondary transmitter. Moreover, when successive decoding is viable at the secondary receiver, rate splitting at the secondary transmitter increases the achievable secondary rate compared to single-user decoding at the secondary receiver.

Another approach is underlay communication systems based on the Ultra Wide Band (UWB) transmission technology. UWB systems rely on the emission of signals characterized by a low power spectral density spread over a wide bandwidth. UWB signals can be broadly divided in the following two families

- Impulse Radio UWB (IR-UWB), where the large bandwidth required to meet the definition of UWB signal set by regulation authorities is achieved by transmitting short pulses (with typical duration in the order of 1 ns);

- OFDM UWB, where the large bandwidth is obtained by transmitting over a wide set of relatively narrowband subcarriers (e.g. 128 4 MHz sub-bands in the WiMedia standard).

Despite the good coexistence capabilities guaranteed by their spectral properties, UWB devices can still have a significant impact on narrowband systems; extensive studies showed for example the potential impact of UWB signals on GPS receivers, and led to the definition of emission masks that forced UWB devices to adopt extremely low power levels in the GPS band [15], [16]. Coexistence capabilities of UWB devices can however be significantly improved by taking advantage of spectrum shaping techniques combined with spectrum sensing, leading to UWB systems that adapt to the interference environment by sculpting the spectrum so to limit or avoid emissions in spectrum bands used by narrowband systems. Both spectrum sensing and spectrum shaping techniques depend of course on the specific characteristics of the selected UWB signal (IR vs. OFDM).

In the case of IR UWB signals the spectrum shaping can be achieved by acting on two key signal components: the code (typically, but not necessarily, a Time Hopping code adopted in combination with a Pulse Position Modulation scheme) or the pulse shape adopted at the transmitter. It can in fact be shown that the Power Spectral Density of the transmitted signal can be written as follows [17], [18]:

$$P_s(f) = \frac{1}{T_s} C(f) \left| P(f) \right|^2 P_x(f) \qquad (2.2.1)$$

where

- T_s is the pulse repetition period adopted in the UWB signal;
- $C(f)$ is the spectrum associated to the code;
- $P(f)$ is the spectrum associated to the pulse;
- $P_x(f)$ is the spectrum associated to the transmitted data x.

Pulse generation in general is a problem widely covered in the literature with respect to implementation efficiency and accuracy, aiming at encoding information in the pulse shape itself: see for example [19], [20]. Moving to the specific problem of addressing coexistence issues by means of pulse shaping, several algorithms for selecting the best pulse shape given external constraints set by regulation and/or interference profiles were proposed in the literature. In [21] an algorithm for the generation of the pulse to be adopted in a Time-Hopping Impulse Radio UWB system was proposed, where a linear combination of pulses obtained as the derivatives of the Gaussian pulse was introduced. A heuristic approach was proposed to determine the values of the coefficients, based on the definition of a emission mask to be met by the transmitted pulse, the mask being the result of constraints imposed by the regulation (e.g., avoiding the GPS band) or resulting from the presence of other wireless services, (e.g. WiMax). Figure 2-1 provides an example of a emission mask taking into account coexistence requirements. The algorithm proposed in [21] generates linear combinations of the base pulses and selects the resulting pulse shape that minimizes the quadratic distance from the emission mask.

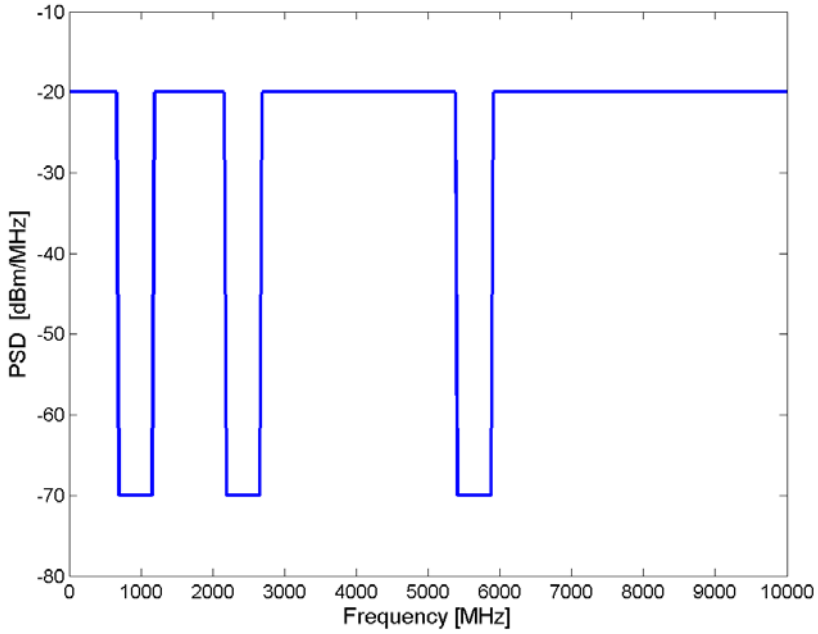

Figure 2-1: Example of emission mask determined by coexistence requirements imposing to avoid ISM bands in the 900 MHz, 2.4 GHz and 5.8 GHz bands.

Authors in [22] face the problem of selecting the pulse by modelling the mask approximation problem as a filter design problem, assimilating the pulse response to a desired FIR filter impulse response. The problem is solved by defining an iterative algorithm based on information exchange between transmitter and receiver that leads to repeatedly execute the Parks-McLellan algorithm for the determination of the required pulse shape, until all constraints set by regulation, interference and synchronization errors are met. In the case of the code, several solutions were proposed in the literature for designing codes that increase the coexistence capabilities of an UWB signal.

Code design adds an additional opportunity to meet coexistence requirements when pulse shaping cannot efficiently be used to address such issue. In [16] authors propose to design the pulse shape so to meet the emission mask set by the FCC, delegating to the code design all additional coexistence constraints, to be met by forcing nulls in the UWB spectrum at frequencies used by other narrowband systems. The code is applied by means of coefficients weighting different Gaussian pulses, so that the coded signal is a weighted sum of such pulses spaced by a pulse repetition period. Authors in [16] show that the proposed approach can be used to generate nulls at desired frequencies while guaranteeing to meet the FCC emission masks.

A different approach was developed in [23], where a spreading code is applied to the phase of the UWB signal, leading to a higher robustness of the UWB link to the presence of narrowband interference by reducing the impact of interferers with carrier frequencies close to the carrier frequency of the UWB link.

Coexistence requirements and capabilities of OFDM-based UWB systems were investigated as well, in light of the definition of the WiMedia industrial standard [24]. MB-OFDM UWB

systems provide a clear advantage over IR-UWB in terms of sensing capabilities. The FFT and IFFT blocks used for the generation and reception of the UWB OFDM signals can in fact be adapted in a straightforward manner to be used for spectrum sensing allowing the UWB devices to determine the presence of coexisting systems with a spectral resolution at least equal to the sub-carrier spacing in the UWB signal. Oppositely, sensing in IR-UWB systems can be more difficult due to the impossibility to identify which specific frequencies over the wide bandwidth of the UWB front-end filter are actually affected by interference.

In [25] the authors analyse the problem of coexistence between MB-OFDM UWB signals and WiMax signals in the 3.5 GHz band. A sensing scheme based on the use of the FFT block at the receiver is proposed, and a-priori information on the spectral characteristics of the uplink WiMax signal (based as well on a OFDM transmission scheme) is adopted in order to formulate the decision problem on the presence of such signal. Results show that high accuracy in detection of WiMax signals can be obtained with a few tens of samples, with a miss-detection probability as low as 10^{-6}.

In [26] a similar application scenario is considered, but the analysis extends to impulsive UWB systems as well, including both Time Hopping and Direct Sequence coded UWB signals. Results presented in [26] suggest that MB-OFDM UWB signals lead to lower interference levels to WiMax receivers compared to both TH-IR-UWB and DS-IR-UWB signals.

Finally, in [27], a coexistence scheme between MB-OFDM UWB devices and IEEE 802.11a networks is proposed. The scheme relies on the sensing feature inherently provided by the MB-OFDM physical layer in order to detect the presence of an IEEE 802.11a network (corresponding to the presence of interference over 5 contiguous sub-bands) and proposes the following two solutions in order to improve coexistence

- An adaptive Frequency Hopping scheme that avoids the bands where the affected sub-bands lie;
- In case all bands are affected by interference (making the adaptive FH scheme ineffective), a selective use of sub-bands, aiming at avoiding the sub-bands impacted by the narrowband interference at the price of a slightly reduced data rate.

2.3 Overlay Cognitive Radio Systems

Cognitive radio systems that have cooperation with the primary system as key feature are typically denoted as overlay cognitive radio system. In general, spectrum overlay refers to the situation where the primary system changes its transmission strategy to involve the secondary system and to set up cooperation. Cooperation between the primary and secondary system can be established for example on the transmitter side or the receiver side.

Transmit cooperation requires that the secondary system is aware of the primary signal parameters and is capable of decoding and processing primary transmissions. Consider the coexistence of primary and secondary links in the context of an overlay cognitive radio (CR) system, where the secondary users try to communicate without disturbing the incumbent primary users. In some scenarios it is reasonable to assume that the secondary transmitter has access to the message sent by the primary transmitter in a non-causal fashion. For

example, whenever the primary transmitter is much closer to the secondary transmitter than to its intended receiver, the capacity of the channel to the former is much larger than that of the channel to the latter. This allows the secondary transmitter to obtain the message in a fraction of the total transmission time. This channel model is known as the cognitive radio channel or the interference channel (IFC) with degraded message sets [28]-[32]. The additional knowledge allows for a form of asymmetric cooperation between the two transmitters. For example, one possible strategy is to have the secondary transmitter employ part of its resources to help the communication between the primary users, so that their communication is not disturbed or is even improved (e.g. in terms of rates). The remaining resources are used for private communication to the secondary receiver. Moreover, with accurate channel state information, the secondary transmitter can use its knowledge of the interference experienced by the primary receiver (or the secondary receiver) to pre-cancel it, for example using dirty paper coding (DPC) [33]. This strategy was shown to achieve capacity in the weak interference regime in [29] and [30]. In contrast, the capacity of part of the strong interference regime was obtained in [31] using superposition coding and interference decoding. In many scenarios the associated capacity gains over non-cooperative transmission could serve as a motivation for having the primary transmitter share its codebook and message with the secondary transmitter [32].

More often, in a typical setup, the primary and secondary systems agree on a cooperative strategy, and the primary system transfers the required information to the secondary system during an initial transmission phase. In [34], [35], it is suggested that a CR can learn the primary message by overhearing primary ARQ transmissions and utilize knowledge of the message to perform spectrum overlay during retransmissions of the primary system. As an alternative [36] and [37] consider explicit cooperation of the primary and secondary systems. In any case, learning the primary message requires the secondary transmitter to be passive for certain duration in time, and it leads therefore inevitably to a rate loss for the secondary system which may lower the attractiveness of overlay strategies. A cooperative transmission (for example using distributed multiple-antenna/space-time and channel coding techniques) is then carried out in a second phase. Depending on the chosen communication strategy the primary receiver may or may not be changed. The primary system potentially gains diversity, throughput, or coverage through this cooperation and can save energy. The secondary system on the other hand can utilize the cooperative transmission for its own purpose and embed own data in the cooperative transmission. A secondary transmitter can for example compensate for and control the interference due to embedded secondary data by spending additional power for the message of the primary system, by using (multiple-antenna) interference cancelation techniques, or by combining both strategies. In this way, secondary transmit opportunities are created. Since the effectiveness of transmitter cooperation is limited by the first initial transmission phase, transmit cooperation is mostly relevant if the primary and secondary transmitters are close and can transfer the primary's message effectively using high transmission rates and low transmit powers.

Receive cooperation can be an alternative strategy if the primary and secondary receivers are close to each other such that they can establish efficient communication among them. In receive cooperation, the secondary system after decoding its own message can forward side information to the primary system. This side information can contain additional

information on the secondary's message which then allows the primary system to decode and cancel out the interference from the secondary, or it can forward a compressed version of its residual signal after decoding, which can be used by the primary receiver to enhance the signal-to-noise-and-interference ratio for the desired signal component. Receiver cooperation can essentially provide the same benefits as transmit cooperation; however, it requires a modification of the primary's receiver while the primary transmitter can (but needs not to) be ignorant to the cooperation.

3. Description of Directives from Decision Engine

This Section corresponds to the similar section in D12.1. In addition to an enumeration of important system and decision parameters, it is described how their instantiation as orders and directives influence the execution algorithm on the physical layer. Special emphasis is put on the constraints and requirements formulated by the decision engine, since it can define the interface between decision and execution. For the discussion on the joint optimization of decision and execution engine see Section 1.

3.1 Mapping directives from network layer to physical layer

In the network layer, end-to-end delay and throughput, mobility management, and traffic classes are metrics important to all the three CR paradigms. How are they mapped to the physical layer is described.

3.1.1. End-to-end delay and throughput

The relation between higher layers and physical layer is often less evident than the one between lower layers and physical layer, but such relation is in any case always present. Several metrics related to network and higher layers were introduced in Sections 2.1.3 and 2.1.4 of [38]. As for network layer, end-to-end delay and throughput were identified as key metrics to determine the performance of the network. In terms of such metrics, performance goals can be defined as a minimum threshold for end-to-end throughput and a maximum threshold on end-to-end delay. Typically, such requirements are fulfilled by the combination of routing and flow control, thus restricting actions to the network layer itself: the actual performance will in this case mainly depend on the network connectivity and on the capacity of the network links. In case of a cognitive wireless network, however, the requirements can be addressed by involving the physical layer as well, thanks to the potential impact of physical layer parameters on network connectivity. Different transmit power levels and, more in general, different transmission parameters (coding, modulation) can lead to different network connectivity and different capacity of the available links.

An optimal solution for maximization of end-to-end throughput should thus take advantage of the possibilities offered by the physical layer, by taking into account potential capacity on each network link. The selection of the optimal route would thus require the selection of transmission parameters for each involved link, and the communications of the choice to the corresponding physical layer so to actually configure the link. The adoption of such a strategy poses however the following open problems

- the amount of information required throughout the network can be too high to be exchanged within a reasonable time with acceptable overhead;
- the stability of information cannot be guaranteed (especially in the case of a cognitive network where unpredictable external factors can change link capacity without control of network devices).

In most cases this will lead to the adoption of suboptimal solutions, such as solutions that take decisions on the basis of local information rather than a global one.

3.1.2. Mobility management

Mobility management, although not traditionally framed in the OSI stack approach, is another function that may pose requirements that can be translated directly in physical layer directives. Depending on the amount of information about mobility patterns of network devices, mobility management may require an adjustment in transmission parameters so to avoid or delay connectivity interruptions.

A decision engine aware of all the relevant information would be the ideal place where to take such decisions. As an example, the combined knowledge of the relative mobility patterns of two devices involved in a communication as well as the remaining time for completing such communication could send a directive to the physical layer so to ensure that connectivity is maintained until the exchange is completed, avoiding thus service interruptions that would be unavoidable without the combination of information coming from different functions at different layers.

3.1.3. Traffic classes

Different traffic classes may impose different constraints on the underlying network. As an example, delay sensitive traffic may lead to the selection of routes involving terminals characterized by low traffic and thus lower delay. Several standards define sets of traffic classes. This is the case for example of the IEEE 802.11e standard [39], where four classes are proposed: Background, Best Effort, Video and Voice. In general, each class is characterized by a different priority, and different transmission parameters at the different layers, from transport (e.g. maximum and minimum value of the contention window) down to MAC (duration of transmission slots) and physical layer (modulation, coding and error protection).

3.2 Mapping directives from MAC layer to physical layer

In the MAC layer, rate requirements, delay requirements, queuing and stability, and fairness are introduced, and how are they mapped to the physical layer is described. These metrics are more difficult to achieve for interweave CR than for underlay or overlay CR, because the secondary users can transmit only when there is vacant spectrum, which is unpredictable.

3.2.1. Rate requirements

The MAC layer provides upper layers services in form of logical channels, which can have different requirements depending on the type of information a logical channel carries (control data or traffic data). It maps as well the logical channels to transport channels provided by the physical layer. It typically determines the transport format, which specifies how data is transmitted over the radio interface. The transport format in conventional wireless systems specifies parameters like channel coding and hybrid ARQ parameters, modulation, as well as antenna and resource mapping. In this way, rate requirements are communicated to the physical layer. Critical parameters are summarized in the following Table 3-1.

Parameter	Representation	Comment
Coding Rate	$R \in [0,1]$	Specifies the rate of the channel code (number of information bits per code bit).
Code	Turbo Code, LDPC Code, Convolutional Code, etc.	Specifies which coding scheme is selected.
Modulation	M-PSK, M-QAM, etc. $M \in [2,4,8,16,\dots]$	Specifies the signal space constellation used to map coded bits into transmitted symbols
H-ARQ	$R_0, R_1, \dots, R_{min}$, with $R_0 > R_1 > \cdots > R_N$	Specifies whether hybrid ARQ is used to resolve transmission errors, gives the maximum number N of retransmissions, and defines a set of rates used for the respective retransmission.

Table 3-1: Transport format from the conventional MAC layer.

Compared to conventional systems, we can expect that the respective parameters in cognitive radio systems can come from larger sets of feasible parameters and have in this sense a higher range. Especially the specification of the radio resources (for example number of carriers, carrier frequencies, carrier bandwidth, etc.) has to be very flexible. Depending on the considered spectrum-sharing paradigm, we can furthermore expect that additional parameters describing transmission constraints need to be handed over. These constraints can for example describe a spectral mask that controls interference to primary receivers in underlay transmissions and limits the out-of-band radiation in interweave and underlay systems. In a similar way, one can define a spatial mask to specify how much power can be radiated into a specific spatial direction if multiple-antenna techniques are used. An example for relevant parameters is given in Table 3-2.

Parameter	**Representation**	**Comment**
Number of Carriers	N_c	Specifies the number of carriers if multi-carrier signalling is used.
Carrier Frequencies	$f_{c1}, f_{c2}, \dots, f_{cN_c}$	Specify the centre frequencies of the carriers[1].
Carrier Modulation	$B_1, B_2, \dots, B_{N_c}$	Specifies the signal space constellation that is used to map coded bits into transmitted symbols
Spectral Mask	$[c_1, \dots, c_{N_M}]$, associated with $[f_1, f_2, \dots, f_{N_M}]$	Specifies threshold values c_k for power levels, etc. at desired frequencies f_k.
Spatial Mask	$[c_1, \dots, c_{N_M}]$, associated with $[\boldsymbol{d}_1, \boldsymbol{d}_2, \dots, \boldsymbol{d}_{N_S}]$	Specifies threshold values c_k for power levels radiated into spatial directions $\boldsymbol{d}_k$.

Table 3-2: Relevant parameters in a cognitive MAC.

[1] Note that the frequencies need not to be orthogonal and that the carriers need not to be ”neighbours”.

While the aforementioned extensions of the MAC layer are rather mild, a significant change is required for overlay spectrum sharing since here interaction with the primary system is required. To illustrate this we discuss in the following changes in the protocol stack that are required to set up transmit cooperation with the primary transmitter. Here, we assume that the primary receiver is not changed; that is, the cooperative transmission has to be transparent to the primary receiver.

We assume that MAC scheduler at the secondary has requested to set up a cooperative transmission with the primary and that the primary transmitter accepts the request. Since the secondary transmitter is typically subordinated to the primary transmitter and interaction is required, part of the scheduling for the secondary transmission is taken over by the primary's MAC scheduler. The primary scheduler provides

- Specification of coding, modulation, and resources (time and frequency) for the initial transmission from the primary transmitter to the secondary transmitter;
- Specification of coding, modulation, and resources (time and frequency) for the primary's message in the second cooperative transmission to the primary receiver;
- Constraints for the embedded secondary message in the cooperation phase (for example interference power constraints for a particular spatial direction if sufficient CSI is available or outage constraints if no or limited CSI is available).

Based on this, the MAC scheduler at the secondary transmitter selects transmission parameters for the secondary's message (channel coding, modulation, multiple-antenna processing) and forwards this information together with the information received from the primary transmitter (primary message and transmit parameters) to the physical layer.

3.2.2. Delay requirements

Delay requirements are taken into account by the scheduler at the MAC layer when parameters for transmission strategies and rates for hybrid ARQ are set. Based on round-trip times and delays on the feedback channel (which can be assumed to be known system parameters) the scheduler can plan how many retransmissions can be carried out for a given rate constraint and which rate allocation minimizes the outage probability. Similarly, initiating cooperative transmissions with other partners can lead to delays which have to be taken into account when scheduling delay-sensitive data. We summarize important parameters in Table 3-3.

Parameter	Representation	Comment
Maximum Delay	D_{max}	Specifies the maximum allowable duration of a transmission.
Round-Trip Time	T_R	Specifies the duration in time for a single transmission and reception of the response by the respective receiver.
Feedback Delay	T_f	Specifies duration in time by which feedback from the receiver is delayed.

Table 3-3: Parameters related to delay requirements.

3.2.3. Queuing and stability

In this subsection, three basic extensions of the usual notion of achievable rate or achievable spectral efficiency are provided in the context of cognitive radio systems. Please refer to Section 2.1.1.2 in [38] for a brief overview on stability, outage and average performance region and the corresponding utility functions for resource allocation.

In order to perform a transmit optimization on the physical layer, we need to define the performance metric effective capacity in detail. In [40], the effective capacity is optimized for a single point-to-point MIMO link with partial channel state information at the transmitter and perfect channel state information at the receiver. Note that the stability region for a primary MAC with single cognitive secondary link is considered in [41].

As indicated in Figure 3-1, the queuing behaviour at the transmitter is considered as well as the precoding and transmit strategy on the physical layer. Dual to the concept of effective bandwidth [43], which models the asymptotic stochastic behavior of source traffic, the concept of effective capacity is developed in [44] to model time-varying fading channels. This performance metric is constructed in order to involve quality of service (QoS) aspects in the resource allocation mechanisms. Determining elements to consider are the queuing behavior of the buffer as well as the asymptotic decay rate of its occupancy [44].

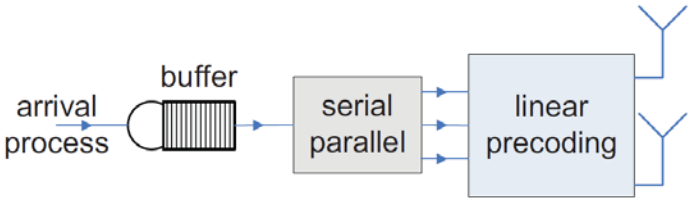

Figure 3-1: Queuing at the transmitter.

The delay, which is a QoS measure, can be described through the probability that the occupancy of the buffer is higher than a specific value, say x. A measure that represents the decay rate of this probability is denoted as the QoS exponent, say θ. This measure is formulated as

$$\vartheta = -\lim_{x\to\infty} \frac{\log \Pr[L > x]}{x}, \tag{3.2.1}$$

where *L* follows the equilibrium queue-length distribution of the buffer at the source [40]. The effective capacity is defined as [45], equation (4)

$$\alpha(\theta) = -\frac{1}{\theta T} \log E\left[\exp(-\vartheta r)\right], \tag{3.2.2}$$

where T is the block-length, r is the random variable describing the transmission rate, and the expectation operator is with respect to r. Given a QoS exponent θ_0, the effective capacity is the maximum constant arrival rate that complies with that QoS constraint. If the arrival rate a satisfies $a \leqslant (\theta_0)$, then the perceived QoS exponent θ satisfies $\theta \geqslant \theta_0$. The performance measure (θ) in (3.2.2) is a generalization of the common performance measure of ergodic capacity and delay limited capacity. For $\theta_0 \to 0$, the effective capacity in (3.2.2) converges to the ergodic capacity. This case corresponds to less stringent delay-constraints.

For $\theta_0 \to \infty$, the effective capacity in (3.2.2) converges to the delay-limited capacity. Therefore, the effective capacity represents an interesting measure which considers non-stringent delay constraints (for finite values of θ_0).

The ergodic capacity (mentioned above for $\theta_0 \to 0$) is often caller average capacity or average rate describes the long-term behaviour of the wireless link, i.e., how many bits can be reliably transmitted over a long (ergodic) time on the fading channel. Using the notation above, it is simply given by E[r]. Note that this performance measure is very rough since neither performance nor delay guarantees can be modeled by the average transmission rate. A finer performance metric is the outage probability. It describes the probability that the system will be in the next channel usage in an outage, i.e., will not achieve the intended transmission rate R. In the notation above it is simple Pr[r<R]. For an overview of average and outage rates, please refer to [46].

In the cognitive radio context, the three different QoS parameters: effective rate, average rate, and outage probability are used to formulate requirements of the decision engine on the execution engine in terms of transmit constraints. The constraints are expressed in two variants. First, for the primary receivers they describe interference constraints. Second, described as QoS requirements for the secondary transmitters. The second scenario is less interesting because it corresponds to the typical transmit optimization under QoS requirements. Consider that the secondary transmitter receives from the decision engine the request to support the QoS requirements of the primary link in terms of average rates *Rp,* outage rates *Ro* or effective rates *Re*, then it is sufficient to maximize the secondary transmission rate under average rate constraints for the primary link. Here, partial channel state information in terms of statistical information is required. The corresponding programming problems are

$$\begin{aligned} &\max R_S \\ &s.t. \quad E[rp] > Rp \\ &or \quad \Pr[rp < Ro] < \varepsilon \\ &or \quad \alpha_P(\theta) > \mathrm{Re} \end{aligned} \tag{3.2.3}$$

where *Rs* is the rate of the cognitive secondary system, and *rp* is the instantaneous primary rate. The instantaneous primary rate depends on the interference created by the cognitive link in the underlay scenario. In the overlay scenario, the instantaneous primary rate depends on the interference as well as the cooperative transmission of the cognitive link.

3.2.4. Fairness

Channel aware and opportunistic scheduling algorithms exploit the channel knowledge and fading to increase the average throughput. Alternatively, each user could be served equally in order to maximize fairness. Obviously, there is a tradeoff between average throughput and fairness in the system. The optimal strategy for maximizing the sum capacity with perfect channel state information (CSI) of a cellular single input single-output (SISO) multiuser channel is to allow only the user having the best channel conditions in terms of SNR to transmit at each time slot (TDMA). The corresponding scheduling policy is called maximum throughput scheduler (MTS) [47]. A major disadvantage of MTS is its unfairness toward users at the cell edge. On the other hand, the most fair but channel unaware scheduler is the round robin scheduler (RRS), that is, all transmissions take place in a strict

numerical order [48]. The MTS and RRS leave room for various channel aware schedulers that lie in between these two. In order to increase the fairness for users at the cell edge, the so called proportional fair scheduler (PFS) can be applied. The PFS weights the instantaneous transmission rates by their averages to find the best user and achieves equal activity probability for all users [49]. Yet another scheduler, which is referred to as opportunistic round robin scheduling (ORS), is a combination of the RRS and MTS [50]. In order to quantitatively measure the impact of the scheduler on the fairness, different measures are proposed. The Jain fairness index (JFI), also known as the global fairness index (GFI), provides a single number between zero and one that measures the fairness even for resource scheduling in finite windows [51]. The average fairness is developed from an information theoretic point of view [52]. The worst-case delay measures the average number of transmissions needed until all users were active at least m times [53]. In the context of cognitive radio, the scheduling fairness of secondary users is more interesting than that of primary users which should be taken care of by the primary system.

3.3 Mapping directives from physical layer to hardware parameters

In the physical layer, spectrum sensing, channel coding and decoding, rate splitting and successive decoding, and channel state information acquisition are introduced, and how are they mapped to the hardware parameters is described. While spectrum sensing is exclusively mandatory for interweave CR, channel coding and decoding is explained specifically for overlay CR. Rate splitting and successive decoding, and channel state information acquisition are more relevant for underlay and overlay CR.

3.3.1. Spectrum Sensing

As previously elaborated in the case of interweave CR systems, the spectrum sensing techniques provide the necessary mechanisms to assess the vacant PU spectrum. In order to perform with high reliability, spectrum sensing techniques must utilize the hardware characteristics of the device in the most efficient manner. This subsection will elaborate the mapping of the physical layer spectrum sensing parameters into the corresponding hardware parameters. The most essential physical layer spectrum sensing parameters are

- **Power of the sensed samples.** This parameter plays a significant role in the detection process of any spectrum sensing technique. For example, in conventional energy detection, the power of the sensed samples is used to decide whether a PU is present or not [1], while in feature detection the samples are used to reconstruct the sensed signal based on which the detection is performed [1].
- **Resolution bandwidth.** It defines the size of the sensed bandwidth. The use of very large resolution bandwidths will give information about wider spectrum range, but can result in accumulating higher noise levels that can degrade the sensing performance.
- **Number of sensed samples.** This parameter relates to the number of samples used for spectrum sensing. Higher number of samples will give higher resolution and fidelity. As already elaborated in section 2.1, higher number of samples can be achieved by either using a higher sampling frequency (device capability) or increasing the sensing time.

- **Sensing time.** The sensing time delineates the period dedicated to spectrum sensing. Higher sensing time can increase the precision of the sensing technique, but can degrade the real-time detection capabilities as well as the throughput of the device.

Table 3-4 describes and elaborates on the mapping between the physical and hardware spectrum sensing parameters.

Physical spectrum sensing parameters	**Hardware parameters**	
	Parameter	***Comment***
Power of the sensed samples	RSSI sampling	**RSSI sampling** is the simplest spectrum sensing approach. Due to its low signal processing complexity, it can be implemented in any sensing device. However, it offers limited options when manipulating the sensed data, thus it is only suitable for energy based detection.
	IQ sampling	**In-phase Quadrature (IQ)** sampling requires higher computational and hardware complexity compared to RSSI sampling, but offers more options for manipulation of the sensed data. The IQ sampling is used in more complex and reliable detection techniques (e.g. FAR, HOS, cyclostationarity based detections etc.)
Resolution bandwidth	Start Frequency and End Frequency	The **Start Frequency** defines the starting point of the sensed band, while **End Frequency** defines the end point of the sensed band. They define the sensed bandwidth window as well as the frequency band being sensed.
Number of sensed samples	Sampling rate /Sweep time/ Sensing points	The **sampling rate** defines how often samples will be taken from the received signal. Increasing the sampling rate will increase the number of sensed samples. For example, in feature detection techniques, higher sampling rate enables better performance of the detection method. The **sweep time** delineates the time needed to cover the whole sensing band. The ratio between the sweep time and the sampling rate gives the number of sensed samples per sweep i.e. the number of **sensing points**. If multiple sweeps are performed, the number of sensed samples will be the product between the sensing point and the number of sweeps.
Sensing time	Number of sweeps /Dwell time/ Sensing points	The **number of sweeps** defines how many times the sensed band will be swept repeatedly. The **dwell time** shows how much time is dedicated per one **sampling point**. Hence, the total sensing time will be defined as the product between the number of sweeps, sampling points and dwell time. In general, higher number of sweeps as well as longer dwell time can increase the precision of the sensing technique, but will increase the sensing time as well.

Table 3-4: Physical to Hardware spectrum sensing parameters mapping

It must be stressed that different spectrum sensing techniques require different settings of the hardware parameters in order to perform the PU detection in the most efficient manner. Hence correct settings of the hardware parameters can prove to be crucial for reliable spectrum sensing.

3.3.2. Channel coding and decoding

In order to discuss the mapping of physical-layer directives into hardware parameters, we consider again the scenario where the secondary transmitter cooperates with the primary transmitter to improve the primary link quality (see e.g. [8][54][55]). We assume that the secondary transmitter performs at the same time an overlay transmission using for example rate splitting, superposition coding, or dirty-paper coding (DPC) techniques as described below. In the following, we focus on channel coding aspects that are important for enabling the cooperation with the primary. We assume therefore that the primary message has already been correctly decoded.

In the considered scenario, the primary transmitter has decided to use a certain implementation of a channel coding technique that is beneficial for the decode-and-forward relay channel. In the literature, different coding schemes like distributed Turbo codes [56]-[58], multi edge type low-density parity-check (LDPC) codes [59]-[61], rate-compatible families of codes (e.g. [62][63]), or fountain codes [64] have been proposed for that purpose. In general, these techniques are closely related to incremental-redundancy hybrid ARQ schemes. Simpler schemes based on conventional point-to-point codes are on the other hand related to ARQ strategies and use for example repetition coding for relaying at the secondary transmitter and maximum ratio combining at the primary receiver.

The choice of the coding scheme typically relies on the amount of channel state information (CSI) that is available at the primary transmitter. If full CSI is available for the channels to the cooperating secondary transmitter and the primary receiver, the primary transmitter can use for example an LDPC code for its transmission to the secondary transmitter, which is then extended in a predefined way by the primary and secondary transmitters in the cooperation phase in order to obtain a good lower-rate code from the initial high-rate code [59]-[61]. In a similar way, distributed Turbo codes can be adjusted to given channel conditions [58]. The general goal of these strategies is to provide incremental redundancy during the cooperative transmission.

On the other hand, if CSI is not available or limited at the primary transmitter, two different strategies may be applied. In the first strategy, the primary selects a code with fixed coderate for the transmission to the secondary transmitter. In the cooperation phase, the primary and secondary transmitter can now either repeat the initial codeword or transmit a new codeword. To maximize diversity if precise channel state information is missing, the message should be decodable (for sufficiently good channels) solely based on the codeword transmitted in the cooperation phase. Note that this may not necessary in the full CSI case where the cooperative transmission is used to provide incremental redundancy instead of the full message. The second strategy that is applicable if CSI at the primary transmitter is missing, is given by the so-call dynamic decode-and-forward protocol [65][66]. In successive retransmissions, the primary transmitter extends the initially transmitted codeword to lower rate codewords by sending incremental redundancy. The secondary transmitter

overhears the transmission, decodes as soon as the rate of transmission is low enough, and starts a cooperative transmission once it has learned the primary message. The cooperative transmission stops if the primary receiver acknowledges successful decoding of the message. This strategy can be implemented, for example, with rate compatible LDPC and Turbo codes or so-called rate-less codes. Since the secondary transmitter becomes part of the primary's transmission and coding strategy, it has to have knowledge of all parameters that describe the realization of the chosen coding scheme. For the different coding schemes discussed above, important parameters are summarized in the following. General parameters related to conventional (point-to-point) channel codes are summarized in Table 3-5, Table 3-6, Table 3-7, and Table 3-8.

Parameter	**Representation**	**Comment**
Block length	N	Number of bits per codeword
Number of information bits	K	Number of information bits per codeword
Code rate	$R = K/N$	Number of information bits per code bit

Table 3-5: General hardware parameters valid for any kind of channel code.

Parameter	**Representation**	**Comment**
Generator matrix	$\boldsymbol{G}$	Set of binary basis vectors that span the codeword space.
Sub-matrices of representing the check matrix	$\boldsymbol{A}, \boldsymbol{B}, \boldsymbol{C}, \ldots$	Efficient encoding requires an efficient decomposition of the generator matrix into sub-matrices.

Table 3-6: Relevant hardware parameters for describing an LDPC code.

Parameter	Representation	Comment
Set of Component Encoders	$\{E_1, \ldots, E_c\}$	Set of generator polynomials that specify the employed recursive convolutional codes. It implies the number of component encoders c.
Set of Interleavers	$\{\boldsymbol{\Pi}_1, \ldots, \boldsymbol{\Pi}_{c-1}\}$	The set of interleavers can be represented by a set of permutation matrices that are used to separate the component encoders. Note that no interleaver is required for the first encoder.
Set of Puncturing Patterns	$\{\mathbf{P}_1, \ldots, \mathbf{P}_c\}$	To adjust the code rates of the component encoders, each component code is punctured as specified by an individual puncturing pattern.
Termination	$t \in \{0,1\}$	Flag bit indicating whether the convolutional codes are terminated or not.

Table 3-7: Relevant hardware parameters for describing a Turbo code.

Parameter	Representation	Comment
Constellation Type	PAM, QAM	Specify signal space constellation
Number of bits per channel symbol	*M*	-
Interleaver	$\boldsymbol{\Pi}_0$	Coding and modulation are typically separated through interleavers to spread burst errors.
Mapping into Frames		After modulation, the data symbols are multiplexed and mapped into frames for transmission.

Table 3-8: Relevant hardware parameters for the modulation and mapping into frames.

For extending an LDPC code to multi edge type code for the relay channel or into a set of rate compatible codes as described above the additional parameters required are given in Table 3-9 [61][63][66].

Parameter	Representation	Comment
Matrices of Additional Check Constraints	$\boldsymbol{\Delta H_1}, \boldsymbol{\Delta H_2}, \ldots$	Higher rate codes are extended to lower rates by adding additional check constraints that lead to additional syndrome bits, which are transmitted during the retransmissions.
Sub-Matrices for mapping Syndromes into Channel Symbols	$\boldsymbol{G_1}, \boldsymbol{G_2}, \ldots$	In DF relaying with perfect CSI, the syndrome bits are protected by another channel code; the matrix $\boldsymbol{G}$ corresponds then to the used generator matrix. If rate compatible codes are constructed, the matrices are full-rank square matrices with special column and row weights.

Table 3-9: Additional parameters for characterizing implementations of LDPC relay codes and rate-compatible LDPC codes.

For extending a Turbo code to distributed Turbo code the additional parameters needed to be known at the secondary transmitter are given in Table 3-10 [58].

Parameter	Representation	Comment
Component Encoder	E_R	Generator polynomials for the component encoder used by the relaying node (i.e. the secondary transmitter).
Interleaver	$\boldsymbol{\Pi}_R$	Interleaver used before encoding at the relaying node.
Puncturing Pattern	$\mathbf{P}_R$	Puncturing used by the relaying node.

Table 3-10: Relevant hardware parameters for extending a Turbo code to a distributed Turbo code.

Rate-compatible Turbo codes are typically obtained from low-rate codes by puncturing and can therefore be characterized by a sequence of puncturing patterns as summarized in

Table 3-11. In a similar way, rate-compatible LDPC codes can be obtained from low-rate LDPC codes.

Parameter	Representation	Comment
Set of Puncturing Patterns	$\{\mathbf{P}_1, \ldots, \mathbf{P}_k\}$	Set of puncturing patterns for constructing rate-compatible codes from low-rate mother codes.

Table 3-11: Relevant hardware parameters for describing rate-compatible codes obtained through puncturing.

Successive decoding of interfering primary signals as described above requires that knowledge of code parameters used by the primary transmitter is available at the secondary receiver. These parameters are identical to the channel code parameters summarized in the tables above. For LDPC codes, however, knowledge of the check matrix $\boldsymbol{H}$ is additionally required for decoding.

3.3.3. Rate splitting and successive decoding

The secondary cognitive transmitters can apply sophisticated precoding techniques in order to improve their own achievable rates as well as to cooperate with the primary receivers and help them to successfully deliver their messages. In this subsection, we discuss information theoretic techniques. Rate splitting can be applied in an underlay, as well as overlay cognitive radio scenario to improve the achievable rate of the cognitive links. Dirty paper precoding can be applied only in overlay cognitive radio scenarios in which the primary messages or codewords are a priori known at the cognitive transmitter. Thereby, both the rates of primary as well as cognitive secondary links are increased.

The basic idea of rate splitting was introduced in [67] for the Gaussian multiple access channel as an alternative to time sharing. The messages at the transmitter are deconstructed in multiple virtual messages which are coded with different codebooks. The codewords are superposed and transmitted. The receiver applies a multiuser detector (successive interference cancellation - SIC) and decodes iteratively the combination of codewords. If the rates of the virtual codebooks are properly chosen, all layers can be successfully decoded and subtracted from the received signal.

In the cognitive radio setting, rate splitting was applied for spectral shaping in [68][69] and for spatial shaping in [14]. Since the primary receiver is assumed to be fixed and not adaptable to the secondary transmissions, it cannot profit from the rate splitting approach. However, the cognitive receivers can decide on the optimal decoding order and obtain gains compared to the case in which only a single Gaussian codebook is applied at the cognitive transmitters. In [38] Section 4.1.3.2, the spatial shaping with rate splitting in underlay cognitive radio is reported.

Dirty paper precoding (DPC) is introduced in [33] as a variant of Gelfand-Pinsker precoding for Gaussian interference. It was applied for the Gaussian broadcast channel. In the broadcast channel the transmitter knows the interference it will create at one user due to the codewords of other users and can pre-cancel this interference. Starting with one user who “sees” all the interference from the other users, it can remove the interference from

this first user created at the second and all following users. Thereby a large part of the interference is reduced. Later it was shown that by this strategy, the capacity region of the Gaussian MIMO broadcast channel is achieved [70].

In the overlay cognitive radio scenario, DPC can be applied at the secondary transmitters as described briefly in [71] Section 4.3.2 and in more detail in Section 4.1 of the deliverable at hand.

The important parameter choices describing the realization of rate splitting and DPC on the physical layer are collected in Table 3-12. Either these parameters are provided by the channel and message aware decision engine or they are found by local PHY optimization.

Rate Splitting	**Parameter**	**Interval**	**Function**
Tx	Tx rates	[0,Rmax]	Rates of different layers, properly chosen to allow SIC at the cognitive receivers
Tx	Power allocation	[0,p_max] $\sum_k p_k \le P$	Power allocated to different layers
Tx	Transmit strategies	BF $\|\mathbf{w}_k\| \le 1$	Beamforming, linear precoding under primary rate constraints
Rx	Decoding order	Permutation {1, …, K}	Optimal decoding order for maximum cognitive achievable rate
DPC	Parameter	Interval	Function
Tx	Primary message	Codeword codebook	Cognitive transmitter needs to know the message/codeword the primary will send
Tx	Precoding order	Permutation {1, …, K}	Optimal precoding order for maximum cognitive achievable rate: Code SU first
Tx	Power allocation	[0,p_max] $\sum_k p_k \le P$	Power allocated to different layers
Tx	Transmit strategies	BF $\|\mathbf{w}_k\| \le 1$	Beamforming, linear precoding under primary rate constraints

Table 3-12: Physical-layer parameter to implement rate splitting and DPC

In the case of the coexistence of one primary link and one secondary link, when the interference from primary transmission at the secondary receiver is weak, single-user decoding (SUD) is deployed at the cognitive receiver. When the interference from primary transmission at the secondary receiver is strong, rate splitting can be deployed at the secondary transmitter and successive interference cancellation (SIC) can be deployed at the secondary receiver to increase the achievable secondary rate. At the secondary transmitter, the secondary message is splitted into two parts. Firstly, the secondary receiver decodes and subtracts the first part by treating the second part message and the primary message as interference. Then the secondary receiver decodes and subtracts the primary message by treating the second part message as interference. At last, the secondary receiver decodes the second part message without interference. When the interference from primary transmission is very strong, then rate splitting is not needed at the secondary transmitter,

the secondary message can be decoded after decoding and subtraction of the primary message at the secondary receiver [14].

3.3.4. Channel state information acquisition

One important issue in cognitive radio systems at the cognitive transmitters is to acquire information about the context, i.e., channel state information from the cognitive as well as the primary receivers. This can be realized by some cognitive pilot channel (CPC). The more information is needed at the transmitter and the more this information has been exact, the more feedback over the CPC is required.

In MIMO OFDM systems, this control overhead and signal processing complexity are quite large, leading to the definition of the so-called time-frequency tiles or chunks [72]. To this end, the physical channel structure divides the available time-frequency resources into tiles. The tiles or chunks are considered two dimensional, and each chunk comprises a number of adjacent subcarriers in frequency domain and a number of consecutive OFDM symbols in time domain as illustrated in Figure 3-2. The application of chunks is wide spread and it is proposed, for example, in [72] for multiple antenna systems. For all subcarriers and all OFDM symbols within the chunk, the same spatial signal processing is applied, reducing the signal processing complexity and the feedback overhead considerably [73]. The concept is illustrated in Figure 3-2.

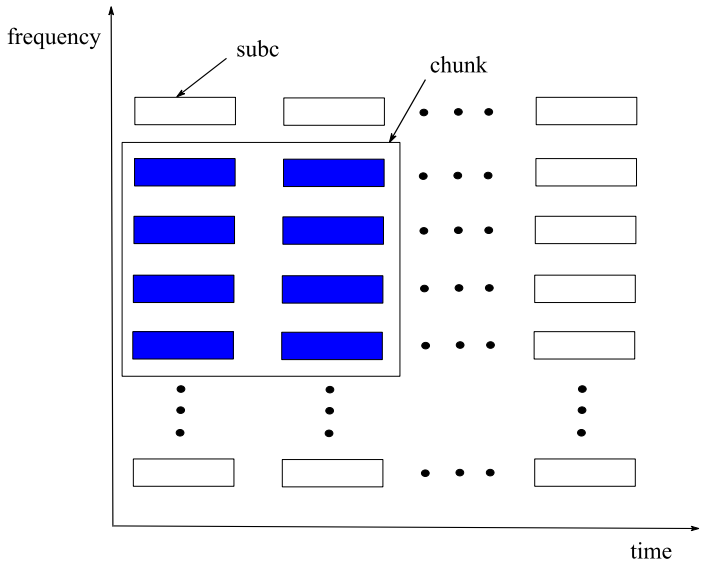

Figure 3-2: Time-frequency chunk.

The optimization of the physical layer with only chunk processing is performed in [72] for the MIMO multiple access channel. The trade off between feedback overhead and performance is studied and an optimal operating point is derived.

Considering the feedback and control overhead in two-link cognitive radio system as illustrated in Figure 3-3 below, the most demanding feedback link is the channel state information from the primary receiver to the secondary transmitter [14].

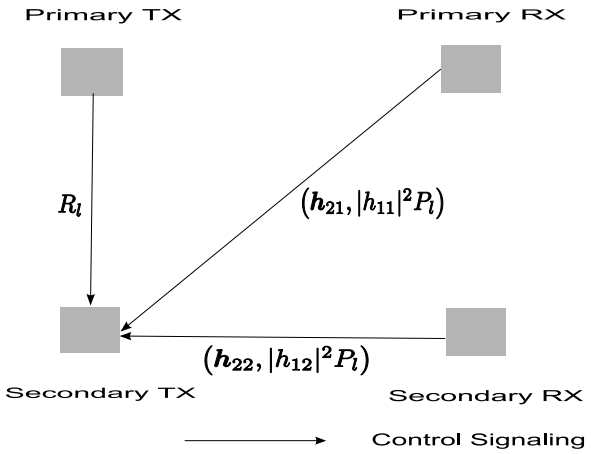

Figure 3-3: Control signalling in two-link cognitive radio system

It will not be possible to feedback this CSI from the primary receiver to secondary transmitter for all carriers. Instead one CSI per chunk has to suffice to optimize the secondary link and to fulfil the primary rate constraint.

4. Description of Signal Processing and Resource Allocation Algorithms

In this section, a collection of signal processing and resource allocation algorithms under different reference scenarios is described. The performance of the algorithms is shown through link-level and system-level simulations. And the complexity of the algorithms is assessed. Moreover, the feedback/control needed for the implementation of the algorithms is analyzed. In Section 4.1, optimal beamforming is proposed for the coexistence of a SISO primary link and a MISO secondary link in overlay CR, where metrics as rate requirements, channel coding and decoding, and channel state information acquisition are involved. In Section 4.2, in the scenario of underlay CR, interference at PUs is limited by utilising spectrum sensing mechanisms while QoS of secondary users are ensured by implementing distributed power control algorithms. In Section 4.3, Time Reversal is proposed for the precoding of UWB signals in underlay CR, where channel state information acquisition is crucial.

4.1 Optimal beamforming in MISO cognitive channels with degraded message sets

4.1.1. System model

Consider the coexistence of primary and secondary links in the context of an overlay CR system. Assuming that the secondary transmitter has access to the message sent by the primary transmitter in a non-causal fashion. One possible strategy is to have the secondary transmitter employ part of its resources to help the communication between the primary users, so that their communication is not disturbed or is even improved (e.g. in terms of rates). The remaining resources are used for private communication to the secondary receiver. Moreover, with accurate channel state information, the secondary transmitter can use its knowledge of the interference experienced by its receiver to pre-cancel it, for example using DPC.

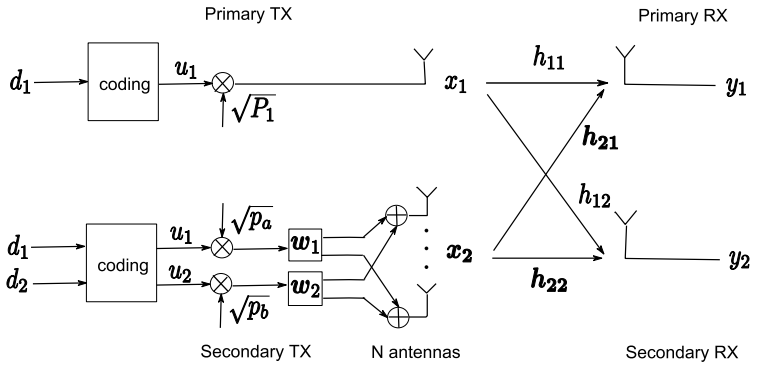

Figure 4-1: System model of primary SISO link and secondary MISO link.

The system considered is depicted in Figure 4-1 and consists of a SISO primary link and a MISO secondary link with N antennas at the transmitter [74]. The primary transmitter conveys a message d_1 with rate R_1 to its intended receiver by encoding it into a codeword

$\mathbf{x}_1$ with an average power constraint P_1. At every time instant the message broadcasted by the primary transmitter is

$$\mathbf{x}_1 = \sqrt{P_1} u_1(d_1) \tag{4.1.1}$$

where u_1 is a symbol with unit average power from the capacity achieving code for a SISO Gaussian channel with a given signal-to-noise ratio (SNR).

Similarly, the secondary transmitter wants to convey a message d_2 with rate R_2 to its receiver. Assuming it has non-causal knowledge of the message d_1, the transmitted codeword $\mathbf{X}_1$ depends in general on both messages. The secondary transmitter has a total power of P_2. A fraction p_a of it is spent in a selfless manner to help the primary-user pair achieve its rate requirement and the rest of the available power p_b (where $p_a + p_a \le P_2$) is used for the transmission of its own message. Furthermore, each of the components has an independent beamforming vector $\mathbf{w}_1$ and $\mathbf{w}_2$, with $\|\mathbf{w}_1\| = \|\mathbf{w}_2\| = 1$. Similarly to the work in [70][75], the secondary user employs superposition coding in combination with DPC. That is, the transmitter employs part of its power to enhance the SNR at the primary receiver. The remaining part of the power is used to convey the message d_2 to its intended receiver, using DPC to protect it against the interference created due to the transmission of the message intended for the primary receiver. The signal broadcasted by the secondary transmitter at a given time instant is therefore

$$\mathbf{x}_2 = \sqrt{p_a}\mathbf{w}_1 u_1(d_1) + \sqrt{p_b}\mathbf{w}_2 u_2(d_1, d_2) \tag{4.1.2}$$

where the secondary transmitter uses the same codebook for d_1 as the primary transmitter, and u_2 is the corresponding symbol with unit average power from a capacity achieving DPC.

The channels are quasi-static block flat fading, and together with the noise components they are modeled as independent and identically distributed complex Gaussian random variables. The channels from the primary transmitter to the primary receiver and the secondary receiver are denoted as h_{11} and h_{12} respectively, with $h_{11} \sim CN(0,1)$ and $h_{12} \sim CN(0,\alpha)$. Similarly, the channels from the secondary transmitter to the primary receiver and the secondary receiver are denoted as $\mathbf{h}_{21}$ and $\mathbf{h}_{22}$, with $\mathbf{h}_{21} \in \mathbb{C}^{N\times 1}$ and $\mathbf{h}_{21} \sim CN(\mathbf{0}, \beta\mathbf{I}_N)$, $\mathbf{h}_{22} \in \mathbb{C}^{N\times 1}$ and $\mathbf{h}_{22} \sim CN(\mathbf{0}, \mathbf{I}_N)$, where $\mathbf{0}$ and $\mathbf{I}_N$ denote the all-zero vector and the $N \times N$ identity matrix, respectively. The noise components at the primary and secondary receivers are denoted as $n_1 \sim CN(0,1)$ and $n_2 \sim CN(0,1)$, respectively.

The following rates are achievable by the primary and secondary users respectively [74]

$$\begin{aligned} R_1 &\le \log_2\left(1 + \frac{|\sqrt{P_1}h_{11} + \sqrt{p_a}\mathbf{h}_{21}^H\mathbf{w}_1|^2}{1 + |\sqrt{p_b}\mathbf{h}_{21}^H\mathbf{w}_2|^2}\right) \\ R_2 &\le \log_2\left(1 + |\sqrt{p_b}\mathbf{h}_{22}^H\mathbf{w}_2|^2\right) \end{aligned} \tag{4.1.3}$$

for any choice of precoding vectors $\mathbf{w}_1$ and $\mathbf{w}_2$ and powers P_1, p_a, and p_b.

4.1.2. Proposed algorithm

The problem of maximizing the transmission rate R_2 for the secondary users while satisfying the rate requirement for the primary link R_1 has the following mathematical formulation [74]

$$\begin{aligned} &\max_{\substack{\mathbf{w}_1, p_a \\ \mathbf{w}_2, p_b}} |\sqrt{p_b}\mathbf{h}_{22}^H\mathbf{w}_2|^2 \\ &\text{s.t.} \quad \frac{|\sqrt{P_1}h_{11}+\sqrt{p_a}\mathbf{h}_{21}^H\mathbf{w}_1|^2}{1+|\sqrt{p_b}\mathbf{h}_{21}^H\mathbf{w}_2|^2} \geq 2^{R_1}-1 \\ &\quad \|\mathbf{w}_1\| = \|\mathbf{w}_2\| = 1 \\ &\quad p_a + p_b \leq P_2,\ p_a \geq 0,\ p_b \geq 0. \end{aligned} \tag{4.1.4}$$

Let $h_{11} = |h_{11}|e^{j\theta}$, we choose

$$\mathbf{w}_1 = \frac{\mathbf{h}_{21}}{\|\mathbf{h}_{21}\|}e^{j\theta} \tag{4.1.5}$$

Given p_a the optimal $\mathbf{w}_2$ can be parametrized as

$$\mathbf{w}_2(\lambda^*) = \sqrt{\lambda^*}\frac{\Pi_{\mathbf{h}_{21}}\mathbf{h}_{22}}{\|\Pi_{\mathbf{h}_{21}}\mathbf{h}_{22}\|} + \sqrt{1-\lambda^*}\frac{\Pi^{\perp}_{\mathbf{h}_{21}}\mathbf{h}_{22}}{\|\Pi^{\perp}_{\mathbf{h}_{21}}\mathbf{h}_{22}\|} \tag{4.1.6}$$

and

$$p_b^* = P_2 - p_a \tag{4.1.7}$$

where

$$\lambda^* = \begin{cases} \lambda_{MRT} & \text{if } \lambda_{\text{MRT}} \leq \dfrac{\text{z}}{\|\text{h}_{21}\|^2\left(P_2-p_a\right)} \\ \dfrac{\text{z}}{\|\text{h}_{21}\|^2\left(P_2-p_a\right)} & \text{otherwise} \end{cases} \tag{4.1.8}$$

$$\lambda_{MRT} = \frac{\|\Pi_{\mathbf{h}_{21}}\mathbf{h}_{22}\|^2}{\|\Pi_{\mathbf{h}_{21}}\mathbf{h}_{22}\|^2 + \|\Pi^{\perp}_{\mathbf{h}_{21}}\mathbf{h}_{22}\|^2} \tag{4.1.9}$$

$$z = \frac{\left(\sqrt{P_1}|h_{11}| + \sqrt{p_a}\|\mathbf{h}_{21}\|\right)^2}{2^{R_1}-1} - 1. \tag{4.1.10}$$

$$\Pi_{\mathbf{h}_{21}} = \mathbf{h}_{21}\left(\mathbf{h}_{21}^H\mathbf{h}_{21}\right)^{-1}\mathbf{h}_{21}^H \tag{4.1.11}$$

$$\Pi^{\perp}_{\mathbf{h}_{21}} = \mathbf{I} - \mathbf{h}_{21}\left(\mathbf{h}_{21}^H\mathbf{h}_{21}\right)^{-1}\mathbf{h}_{21}^H \tag{4.1.12}$$

(4.1.4) can be solved by varying p_a from 0 to P_2 to find the optimal λ that achieves the maximum objective value.

4.1.3. Algorithm performance

In the simulation, the achievable secondary rate of the scenario described is shown, together with that of uninformed secondary link without access to the primary message as in [14], with varying SNR and primary rate requirement. For the underlay CR scenario in [14], rate splitting and successive decoding is deployed when it is viable, otherwise single-user-decoding is used. The loading factor is defined as the ratio of primary rate requirement and

instantaneously achievable primary rate without secondary transmission. For simulation, we set P1 = 10dB and $\alpha = \beta = 0.5$.

As shown in Figure 4-2 and Figure 4-3, for a certain primary rate requirement, secondary antenna configuration, and transmission power, the cooperative transmission strategy derived has a gain over the non-cooperative one in terms of achievable secondary rate [74]. In particular for highly loaded primary links, the gains are tremendous (e.g. for three transmit antennas and 12 dB SNR more than 2 bits per channel use (bpcu), almost a 50% gain for 100% load). Interestingly, for three transmit antennas, the achievable rates with informed cognitive transmitter (as proposed) with 100% load are higher than with uninformed cognitive transmitter (using rate splitting) with 25% load. This clearly indicates that the knowledge of the primary message at the cognitive transmitter helps significantly.

Another observation comparing Figure 4-2 and Figure 4-3 is that with sufficient transmit antennas, the impact of primary link load on the performance of the informed cognitive link is small (less than 0.5 bits per channel use). Finally, at high SNR, the slope of the achievable rate of the rate-splitting scheme and that of the proposed scheme seem to be different. It would be interesting to study the high SNR behavior of the proposed scheme and compare it with the slope achievable for the completely cooperative scheme, i.e. MIMO with two transmit antennas, which has a slope of two.

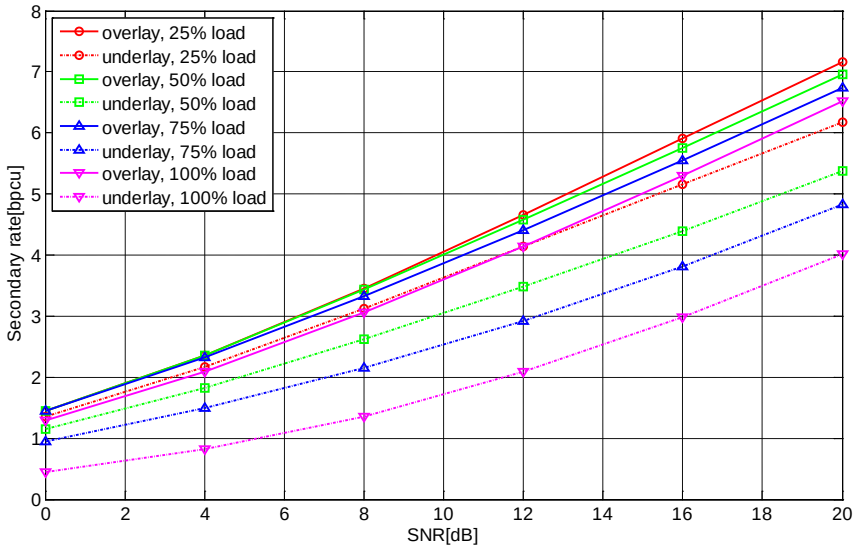

Figure 4-2: Comparison between underlay and overlay multiple input single output cognitive radio link with different loading factors for primary system - two transmit antennas at CR.

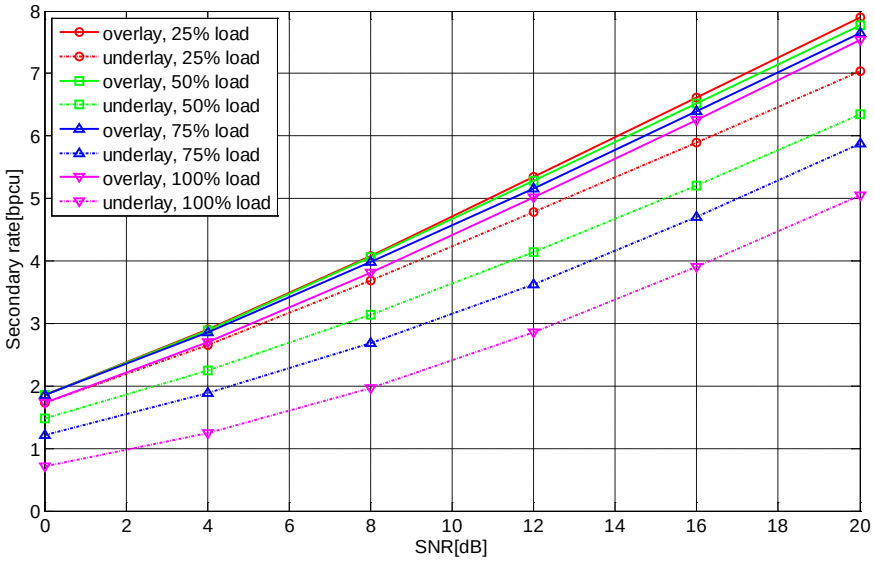

Figure 4-3: Comparison between underlay and overlay multiple input single output cognitive radio link with different loading factors for primary system - three transmit antennas at CR.

4.1.4. Algorithm analysis

In some scenarios it is reasonable to assume that the secondary transmitter has access to the message sent by the primary transmitter in a non-causal fashion. For example, whenever the primary transmitter is much closer to the secondary transmitter than to its intended receiver the capacity of the channel to the former is much larger than that of the channel to the latter. This allows the secondary transmitter to obtain the message in a fraction of the total transmission time.

Clearly, utilizing the knowledge of the primary message at the secondary transmitter comes at the price of overhead. Moreover, given the complexity of DPC, implementation of DPC with low complexity or linear precoding can be considered. The trade off between complexity and performance should be addressed.

The secondary transmitter should get the primary message, transmit power and rate requirement. The primary receiver and secondary receiver should feedback the related CSIs to the secondary transmitter.

4.2 Distributed power control for cognitive radios with primary protection via spectrum sensing

4.2.1. System model

In modern wireless systems, spectrum is allocated on a fixed term basis to transmitters covering a geographical domain. Many studies have shown that not all frequencies are used at every point in time and space, resulting in the underutilisation of the spectral resource [76]. Therefore the problem of spectrum scarcity is clearly not a dearth of spectrum but the inefficient way of spectrum usage caused by static allocation of resources. The idle spectrum in a particular spatial-temporal domain is called spectrum hole. Devices like cognitive radios

(CRs), therefore seek opportunistic use of such spectrum on a non-interfering basis to the spectrum owners called the primary user (PU). The key challenge is to re-use spectrum holes such that primary networks are protected from interference and that the quality of service (QoS) of the cognitive users (i.e. the secondary users) is guaranteed. Transmit Power Control (TPC) is a well-established technique for mitigating interference in wireless networks [77][78][79][80]. However, in cognitive radio networks (CRN), TPC is challenging due to the strict interference avoidance constraints on PUs. In [81] a model based on graph theory was presented while [82] addressed channel allocation problem using game theory. However, PUs were not explicitly protected in these approaches due to opportunistic access of CRs. Recently, there has been a flurry of research considering protection of PUs (e.g. see [82] and references therein). To protect PUs, the transmit power of the CRs should be limited based on its proximity to PUs [83]. However, in realistic scenarios, primary user location is difficult to obtain. Spectrum sensing has been identified as one of the key enablers in the realisation of a true cognitive system [76]. As most of the spectrum sensing techniques are based on transmitter detection, unfortunately spectrum sensing solely does not guarantee absolute interference free operation to the licensed users. We therefore empower the CR to perform TPC, whereby the power control actions are based on spectrum sensing results to prevent exacerbated powers propagating into unwanted primary domains whist maintaining substantial QoS within its own network. Power control based on spectrum sensing information has been discussed in [84] for the case of a single secondary user. However, in future CRNs larger numbers of secondary transmitters and receivers can be expected, and further, the need to provide QoS within this resulting secondary network should also be maintained at the same time.

In this subsection, we extend the approach presented in [84] for the case of multiple secondary transmitter and receiver pairs by enforcing tight bounds on the QoS of both primary and secondary users. QoS is translated to the maximum permissible interference limit (ITL) at the primary receivers while QoS of secondary users is ensured by maintaining its Signal-to-Interference-Noise ratio (SINR) (or Bit Error Rate) above to a predefined threshold. The complexity of the proposed algorithm is as the same level as classical distributed power control and convergence.

We show that interference at PUs can be limited, or at least maintained by utilising spectrum sensing mechanisms while QoS of secondary users can be ensured by implementing modified versions of distributed power control algorithms. In distributed power control algorithms, a user controls its transmitted power by utilising local information only following some power updating rules [79][80]. However, in CRNs with explicit primary user protection, it is difficult to implement classical distributed power control algorithms since the total interference level at PUs can not be identified by the local information. Approaches employing feedback reporting from sensors localised in the vicinity of the primary receiver [85] or genie aided [86] solutions are prone to inherent failures and delays therefore the primary user experiences transient interferences which may be unpleasant.

Autonomous distributed power control algorithm was developed in the CR context [87] with interference consideration to the primary receiver. In this subsection, we focus on distributed power control mechanisms without feedback reporting and employ spectrum

sensing algorithms to derive its link gain to the worst-case location of the PU. The solutions advanced in this subsection leads to a truly distributed framework for cognitive radios while ensuring that the interference environment of the primary user is un-perturbed at all times. In this subsection, the cognitive radio harnesses the spectrum sensing capabilities while implementing the modified distributed power control algorithms proposed in [87] with the following improvements

- The cognitive radios perform localised spectrum sensing of primary TV signals and make individual decisions about their interference environment and link gains to the primary system.
- Increased number of supported CR users is expected since different constraint is executed at individual terminals rather the same constraint being applied to all CR devices as in [87].

4.2.2. Proposed algorithm

Conventional distributed constrained power control (DCPC) and generalized distributed power control (GDPC) algorithms do not guarantee primary user protection; therefore it becomes imperative to modify these algorithms in order to protect the primary receivers. Autonomous distributed power control algorithm was developed in [87] guaranteeing interference free operation to the primary at all times. This algorithm is simple yet effective since CRs communication is possible even at close proximity to the users without raising the interference at the primary user beyond limits. If the ITL threshold ξ_{nl}^{th} and the number of transmitting CRs are known (e.g. using some routing protocol [85][90]), a further cap on the maximum individual cognitive power P_i^{cap} can be can be conditioned as

$$P_i^{cap} \le \frac{\xi_{nl}^{th}\, d_{tv,i}^{\alpha_{cr}}}{N} \quad i \in \{1,2,.....N\} \tag{4.2.1}$$

Since each of the CR users is now constrained by (4.2.1), the ITL at the primary receiver is never violated at any distance from the worst-case primary receiver. The simulation in [87] implicitly considered $d_{tv,i} \approx d_{tv}$ for all CRs, it follows that the same P_i^{cap} constraint would be applied to all N transmitting CRs, which is quite conservative. In our model, we relax this assumption by empowering each CR user with spectrum sensing capabilities such that CR users explicitly determine their respective link gains to the primary receiver and as such compute their respective power constraints. Therefore, CRs in the boundary region of the *m* x *m* block, further away from the primary user, would ideally, contribute lesser interference power to the primary user than CRs in close proximity. A CR transmitter at such boundary locations may therefore be able to communicate effectively with its receiver due to a little more predisposed power achievable depending on its true distance to the primary receiver without violating the ITL. We therefore briefly describe the explicit determination of link gains and formulate the transmission power for CRs.

A. Explicit Estimation of Distance d_i

In order to estimate distance d_i each CR performs spectrum sensing (measures energy Y_i) in *T* number of time slots and calculate $I(Y_i^k)$ in each time slot such that

$$I(Y_i^k) \approx \begin{cases} 1, & Y_i^k \ge \lambda \\ 0, & otherwise \end{cases} \quad i = 1,...,N \text{ and } k = 1,....,T \tag{4.2.2}$$

Hence estimated probability of detection $\hat{P}_{d,i}$ for i^{th} CR is

$$\hat{P}_{d,i} = \frac{1}{T}\sum_{k=1}^{T} I(Y_i^k) \quad for\, i = 1,\ldots,N \tag{4.2.3}$$

Once the probability of detection is estimated, an estimate on the distance from the i^{th} CR to the primary transmitter can be derived based on the closed form expression as

$$P_{d,i} = \frac{\Gamma\left(m-1,\frac{\lambda}{2}\right)}{\Gamma(m-1)} + \left(1+\frac{1}{m\,\overline{\gamma}_{tv,i}}\right)^{m-1}\left(e^{-\frac{\lambda}{2(1+m\overline{\gamma}_{tv,i})}}\right)\left(1-\frac{\Gamma\left(m-1,\frac{\lambda m\overline{\gamma}_{tv,i}}{2(1+m\overline{\gamma}_{tv,i})}\right)}{\Gamma(m-1)}\right) \tag{4.2.4}$$

Since $\hat{P}_{d,i} \approx P_{d,i}$, it suffices to have $\hat{D}_i \approx f^{-1}(1-P_{m,i})$. It is then possible to plot the graph of probability of missed detection with estimated distance $\hat{d}$ as in Figure 4-4 [84], which shows how the probability of missing a primary signal varies with distance from the primary contour for various primary transmitter powers. The lower the primary transmission powers the better the opportunity for CRs. The improved maximum individual CR power is given in

$$P_i^{cap} \le \frac{\xi_{nl}^{th}\; f^{-1}(1-P_{m,i})}{N} \quad i \in \{1,2,\ldots\ldots N\} \tag{4.2.5}$$

We therefore modify the DCPC and GDPC algorithms to include spectrum sensing capabilities and call them DCPC/GDPC with Primary Protection via Spectrum Sensing.

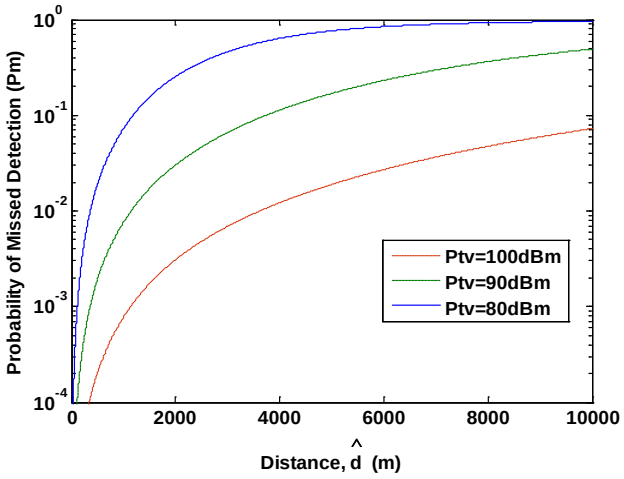

Figure 4-4: P_m vs. $\hat{d}$ for P_{fa} = 0.01 and m=5.

B. DCPC with Primary Protection via Spectrum Sensing (DCPC-PPSS)

The DCPC-PPSS algorithm advanced here implements spectrum sensing to estimate its distance to the primary receiver. The iterative power process is therefore written as

$$P_i(t+1) = \min\left\{\frac{\gamma_{cr}^{th}}{\gamma_{cr,i}^{t}}P_i,\ \frac{\xi_{nl}^{th}\; f^{-1}(1-P_{m,i})}{N},\ P_{\max}\right\}, \quad t \in \{0,1,,\ldots\} \tag{4.2.6}$$

When the CRs are sufficiently far from the primary system, equation (4.2.6) would tend to increase making $P_i^{cap} \ge P_{\max}$, hence (4.2.6) ensures that the CR never exceeds its maximum available power.

C. GDPC with Primary Protection via Spectrum Sensing (GDPC-PPSS)

The GDPC-PPSS algorithm implemented here is similar to the DCPC-PPSS algorithm in that they both implement the same mechanism. However, like conventional GDPC algorithm, GDPC-PPSS has the ability to support an increased number of CR transmitters compared to the DCPC-PPSS. The power updating rule for GDPC-PPSS is as in (4.2.7).

$$P_i(t+1)=\begin{cases}\dfrac{\gamma_{cr}^{th}}{\gamma_{cr,i}^{t}}P_i(t) & if \quad \dfrac{\gamma_{cr}^{th}}{\gamma_{cr,i}^{t}}P_i(t)\le \min\left\{\dfrac{\xi_{nl}^{th}\ f^{-1}(1-P_{m,i})}{N},\ P_{\max}\right\}\\ \hat{P}_i & if \quad \dfrac{\gamma_{cr}^{th}}{\gamma_{cr,i}^{t}}P_i(t)> \min\left\{\dfrac{\xi_{nl}^{th}\ f^{-1}(1-P_{m,i})}{N},\ P_{\max}\right\}\end{cases} \tag{4.2.7}$$

where $t\in\{0,1,2,....\}$ and $\hat{P}_i$ is an arbitrary power value.

4.2.3. Algorithm performance

Simulation parameters are given in Table 4-1. For ease of presenting our simulation result, we estimate

$$\hat{d}=\frac{1}{N}\sum_{i=1}^{N}\hat{D}_i-r_{nl} \qquad i=1,...,N \tag{4.2.8}$$

Simulation results in Figure 4-5 show that by implementing the proposed algorithm, ITL at primary receivers is never exceeded. It also shows that the interference powers of the CRs decreases significantly as the CRN moves further away from the noise limited contour of the TV receiver. The number of supported users is expected to increase with further distance from the primary contour as shown in Figure 4-6. DCPC-PPSS experiences a slight decline at an estimated distance of 2500m due to increased maximum power available for to each user, however GDPC-PPSS tries to maintain the number of supported CR users. The algorithm is seen to stabilize with distances greater than 2500m owing to reduced downlink intersystem interference from TV transmitter. GDPC-PPSS supports more number of than DCPC-PPSS due to reduced interference levels experienced in the network.

Simulation Parameters	Values
Primary Transmit Power (P_{tv})	80dBm
Effective Coverage range of TV statation (r_{nl})	70Km
Noise power for 8MHz UK TV channel	-105dBm
Interference level at r_{nl}	-100dBm
Number of CR Transmitters (N)	50
CR maximum terminal power (P_{max})	20dBm
CR coverage area	2000m x 2000m
Pathloss exponent for primary (α_p)	3
Pathloss exponent for CR transmitter (α_{cr})	4
Distribution of CR terminals	Random($r_{i,i}\geq r_{i,j}$)
Probability of false alarm (P_{fa})	0.01
Time bandwidth product (m)	5
Arbitrary power $\hat{P}$	0dBm
No of time slots for sensing operation	1000

Table 4-1: Simulation parameters for fully distributed CRN.

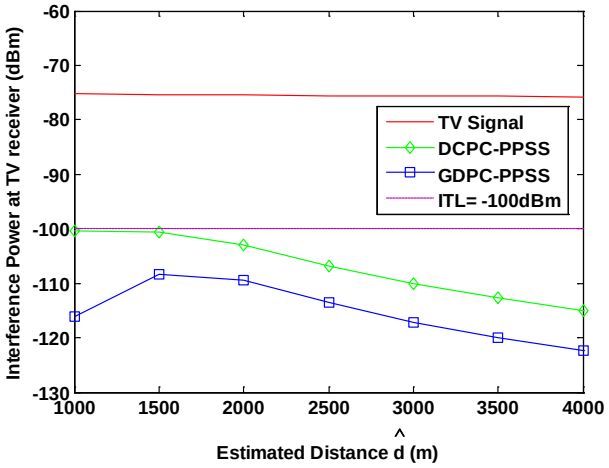

Figure 4-5: CR interference power with estimated distance.

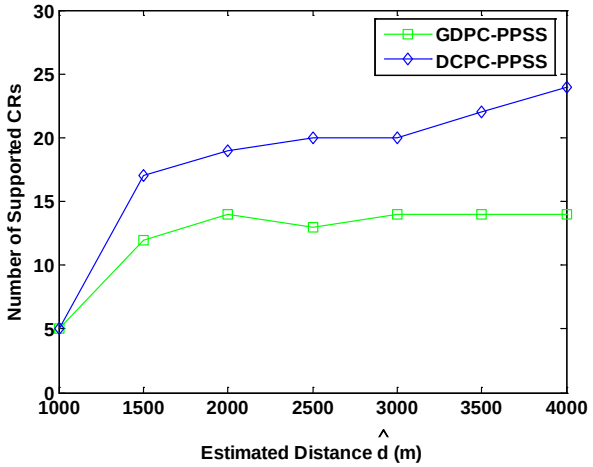

Figure 4-6: Supported CR transmitters with estimated distance.

4.2.4. Algorithm analysis

DCPC/GDPC-PPSS offers a more realistic model for a fully distributed CRN framework since power control and link gain estimation (achieved through spectrum sensing) are performed at the individual CR terminal without any co-operation or co-ordination from the primary system. We have therefore been able to re-use the primary TV spectrum owing to spatial opportunity while ensuring that the total transmission power of CR users in all TV channels does not exceed the interference threshold limit at the worst case primary receiver at any time. DCPC/GDPC-PPSS are a viable approach as fully distributed schemes for the cognitive radio framework.

4.3 Precoding of UWB signals by Time Reversal

4.3.1. System model

Time Reversal (TR) is a technique borrowed by acoustics [91], [92] and recently applied in wireless communications, mostly combined with Impulse-Radio Ultra Wide band (IR-UWB) [93]. The basic idea behind TR relies on the use of a pre-filter (or pre-coder) in transmission

with impulse response given by the time-reversed version of the channel impulse response (CIR), whose principal effect is the time-space focusing

- **time focusing**: received signal is the auto-correlation of the CIR (convolved with the basic pulse), aptly scaled to meet power constraint;
- **space focusing**: any point of the space but the focused one (where the receiver is located) see a cross-correlation between two (almost) independent channels, so the signal does not show any peak [94].

Our research in this field addresses communications as well as positioning issues. The main results on these topics are

- **energy gain**: receiver can gather more energy with TR;
- **more leptokurtic MUI**: impulsiveness of the multi-user interference (MUI) term in the correlation metrics (after matched filter and sampler at symbol rate) increases with TR;
- **enhanced DOA estimation**: overcoming limitations on subspace decomposition techniques, such as MUSIC, TR becomes a feasible approach for positioning in random and highly frequency-selective media.

We will consider TH-IR UWB (Time Hopping Impulse Radio Ultra Wide Band) signal using PAM (Pulse Amplitude Modulation) as well as PPM (Pulse Position Modulation). The classical (no TR) IR-UWB signal with PAM may be written as follows

$$\mathrm{s(t)} = \sqrt{\mathrm{E_s}} \sum_{\mathrm{k \in Z}} \mathrm{a_k p(t - kT_s - c_k T_c)} \tag{4.3.1}$$

while for PPM modulation, one has

$$s(t) = \sqrt{E_s} \sum_{k \in Z} p(t - kT_s - c_k T_c - b_k \varepsilon) \tag{4.3.2}$$

where

- $p(t)$ is the unit-energy basic pulse waveform;
- E_s is the energy of $s(t)$;
- a_k is the k^{th} symbol to be transmitted in the PAM case;
- b_k is the k^{th} bit to be transmitted in the PPM case (thus $a_k = 2b_k - 1$);
- T_s is the slot duration;
- T_c is the chip duration.

In the following analysis perfect channel information both at the transmitter (CSIT) and at the receiver (CSIR) is assumed.

4.3.2. Proposed algorithm

The principle of Time Reversal is to convolve the pulse by an inverted version of the channel before to send it. So, the propagation of the signal through the channel will have the effect to receive the channel correlated to itself (thus simulating a correlation receiver). The transmitted signal in case the precoding TR technique is adopted writes for both PAM and PPM cases, respectively, as

$$s^{TR}(t) = \sqrt{\frac{E_s}{\int |h_{in}(t) * p(t)|^2 dt}} \sum_k a_k h_{in}(t) * p(t - kT_s - c_k T_c) \tag{4.3.3}$$

$$s^{TR}(t) = \sqrt{\frac{E_s}{\int |h_{in}(t) * p(t)|^2 dt}} \sum_k h_{in}(t) * p(t - kT_s - c_k T_c - b_k \varepsilon) \qquad (4.3.4)$$

where signals were normalized so to meet the power constraints. In the above equations $h_{in}(t)$ is the precoding filter, that in case of perfect Time Reversal satisfies the condition $h_{in}(t) = h(-t)$.

Note that the precoding TR filter at the transmitter can be combined with a rake receiver to take into account the typical multipath environment for UWB signals. Either an all-rake or a partial rake receiver can be adopted, depending on the desired trade-off between receiver complexity and performance. In general, one can achieve a global trade-off by tuning the number of taps N_{in} used in the TR precoding filter with the N_{out} fingers used in the rake receiver.

4.3.3. Algorithm performance and analysis

In order to illustrate the time and space focusing properties guaranteed by TR, one can consider the following scenario: two transmitters, say TX_1 and TX_2, communicating to their reference receivers, say RX_1 and RX_2 respectively. Denote by CIR_{xy} the channel between TX_x and RX_y, and by $RCIR_{xy}$ its time-reversed version. Accordingly, denote by $r_{xy}(t)$the signal received by RX_y and transmitted by TX_x.

Time focusing

The focusing in time is of particular interest for Impulse Radio UWB, as Impulse Radio UWB is primarily designed to work with focused pulses in time (i.e. ultra short pulses). TR helps in refocusing the signal in time by compensating for the spreading effect caused by the presence of a multipath channel between transmitter and receiver. Time focusing follows from the property that the auto-correlation function (ACF) of a signal shows a narrow peak (with amplitude equals to its energy).

If a transmitter uses TR, say TX_1, the transmitted signal is given by the convolution of the basic pulse with $RCIR_{11}$ (scaled by a factor that guarantees the power constraint), and the signal received by the reference receiver is further convolved with CIR_{11}. The convolution of $RCIR_{11}$ and CIR_{11} gives the ACF of the latter, and shows a narrow peak.

Space focusing

Space focusing follows from the statistical independence of cross channel impulse responses, i.e. CIR_{xy} with x different from y. In that case, CIR_{xy} is the cross-correlation of two independent processes and the ACF's property of having a narrow, tall peak does not hold anymore.

Thus TR focuses a signal in one point in the space, corresponding to the position of the reference receiver, helping to reduce interference generated to receivers in different positions.

Effects on communications

The first major effect is the energy gain achieved with TR. In other words, e.g. for PAM, the energy received at the reference receiver in correspondence of the signal with TR defined in (4.3.3) is greater than the energy received when the signal without TR defined in (4.3.1). The same is true with PPM. It can be shown analytically that this property is irrespective of the modulation type, as it only depends on the channel statistics [95].

Table 4-2 shows the efficacy of the different combinations of TR and rake receiver, defined as energy per pulse captured by the receiver, with respect to the available energy at the receiver input without TR for the same transmitted energy, for a system with N_{in} taps and N_{out} fingers.

N_{out}	N_{in}=1	N_{in}=10	N_{in}=20	N_{in}=all
1	14.8 %	54.5 %	75 %	100 %
10	55 %	81.8 %	98.8 %	120.3 %
20	75.2 %	94 %	112.1 %	132.4 %
all	100 %	144.2 %	165.2 %	191.6 %

Table 4-2: Efficacy - energy per pulse captured by the receiver, with respect to the available energy at the receiver input without TR for the same transmitted energy.

Figure 4-7 present additional data on efficacy of the combination of TR with rake. The channel used in simulations is the CM1 (LOS) of IEEE 802.15.3a.

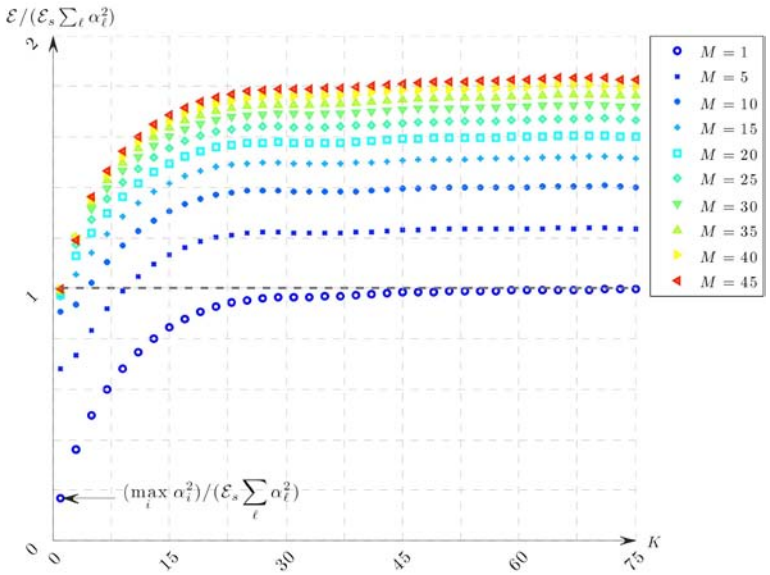

Figure 4-7: Efficacy - energy per pulse captured by the receiver, with respect to the available energy at the receiver input without TR for the same transmitted energy with partial TR (K=Nin taps) and RAKE (M=Nout fingers).

The second major effect is the increase of the non-Gaussianity of MUI, measured by the kurtosis of the MUI term after correlation and sampling (i.e. of the data set of the MUI term within correlation metrics). This effect is mostly due to the impulsiveness of the MUI signal at the receiver. While the non Gaussianity of the MUI is a problem when a classical receiver is used, it has been shown in [96] that, for the same MUI, performance increases as the non

Gaussianity of MUI becomes more pronounced when adopting an adapted receiver. So, we show a new advantage of TR in addition to the usual ones: the fact that TR increases the non Gaussianity of the MUI. Figure 4-8 shows that the more leptokurtic is the MUI term, the better the performance of the overall system when an adapted receiver is adopted.

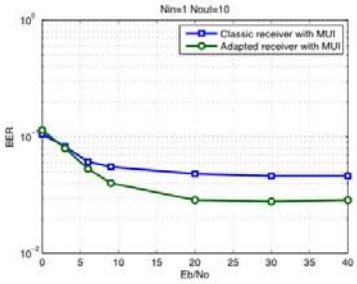

(a) BER vs. SNR with $N_{in} = 1, N_{out} = 10$

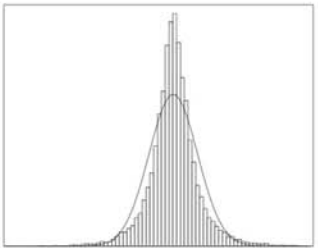

(b) $Kurtosis = 3.5$

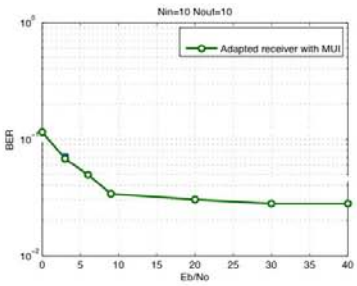

(c) BER vs. SNR with $N_{in} = 10, N_{out} = 10$

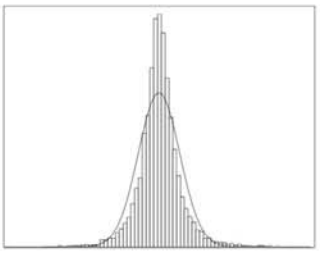

(d) $Kurtosis = 4.1$

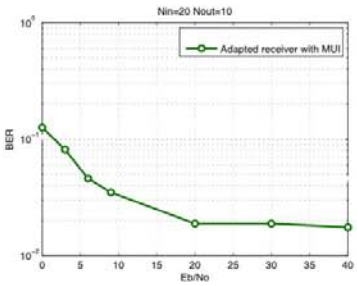

(e) BER vs. SNR with $N_{in} = 20, N_{out} = 10$

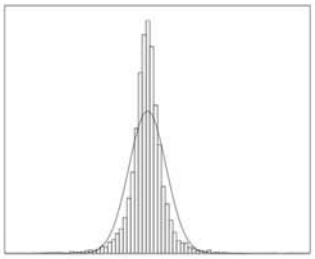

(f) $Kurtosis = 9.8$

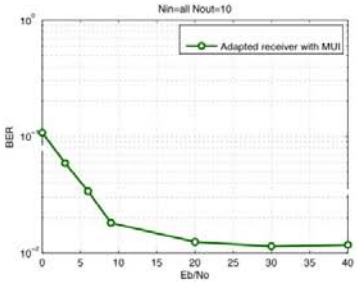

(g) BER vs. SNR with $N_{in} = all, N_{out} = 10$

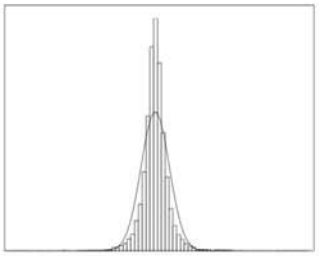

(h) $Kurtosis = 17.6$

Figure 4-8: Bit Error Rate performance (left); Histograms showing the distributions of the MUI term and superposition with a Gaussian probability density function having the same variance in order to underline the non- Gaussianity (right).

Effects on positioning

In addition to the benefits on communications discussed in previous subsection, the impact of Time Reversal combined with UWB on positioning was addressed. UWB and TR can provide significant benefits to positioning accuracy in presence of harsh channel conditions due to frequency selective and dishomogeneous propagation media. The issue was addressed in [96] for a scenario characterized by a positioning device equipped with an antenna array composed of *m* elements aiming at positioning *d* targets in unknown positions by means of Direction of Arrival (DOA) positioning, as shown in Figure 4-9.

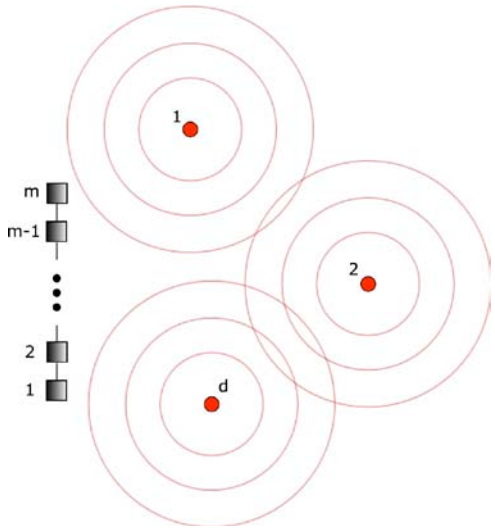

Figure 4-9: Application scenario considered in the analysis of the application of UWB and Time Reversal to positioning.

The problem of determining the angle of arrival of a signal by means of an array of antenna elements was studied extensively by the research community, and several solutions were proposed. A well known approach relies on subspace decomposition of a covariance matrix built on the basis of the signal received on each antenna array element from the targets to be located: this was the basis for the definition of the MUSIC algorithm [97].

The MUSIC approach presented above works in a very efficient way when an accurate description of the relation between the angle of arrival θ and the signal present at each array element is available. This is the case for homogeneous propagation media, for which a very good approximation of the impact on each array of a signal coming from an arbitrary point in space can be achieved by means of planar wave assumption. In the case of not homogeneous media the MUSIC approach applied to the covariance matrix leads to poor results, due to the lack of accuracy in modeling the propagation of the signals. The combination of the MUSIC approach with the Time Reversal technique leads in this case to improved results, as shown in [98], where a solution combining Time Reversal and MUSIC in the time domain is proposed, capable of guaranteeing high positioning accuracy in random media as well.

In this context, the adoption of UWB can further improve the performance of a positioning system, by reducing the impact of spurious peaks in the MUSIC pseudospectrum due to low SNRs of the signals arriving at the array at a specific frequency. As an example, let us

consider the scenario presented in Figure 4-10, where an array of 9 elements is used to determine the direction of arrival of signals emitted by two targets. Figure 4-11 presents the results obtained by applying TR and MUSIC to narrowband signals at frequency f_p = 3.5 GHz under ideal conditions without thermal noise, and highlights the very good performance of the algorithm, with virtually error-free estimation of direction of arrival of the two signals. Figure 4-12 presents the results obtained under the same hypothesis about signal bandwidth, but in presence of thermal noise and assuming a SNR of 10 dB for both signals, reduced by 10 dB due to an additional path loss introduced over a 50 MHz band centered around f_p. The figure highlights the low accuracy of the algorithm under these conditions. Finally, Figure 4-13 presents the results obtained by replacing the narrowband signals with UWB signals characterized by a 500 MHz bandwidth around f_p, Results show the potential improvement achieved by taking advantage of larger bandwidths when dealing with frequency selective channels.

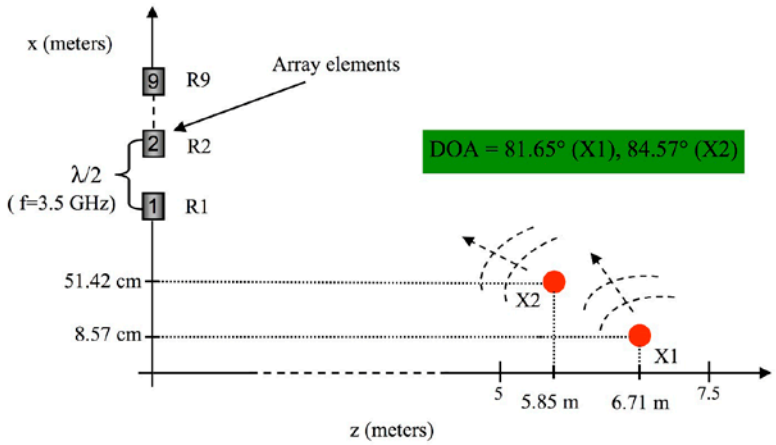

Figure 4-10: Simulation scenario used as an example of application of TR and MUSIC to UWB signals.

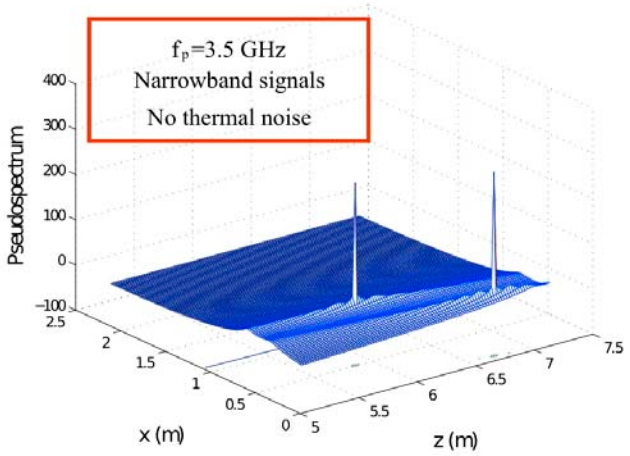

Figure 4-11: DOA estimation obtained in absence of noise by applying TR and MUSIC to narrowband signals at f = fp.

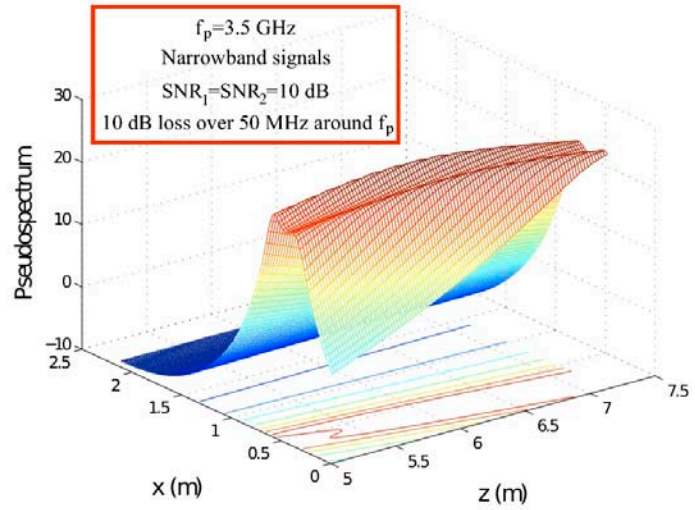

Figure 4-12: DOA estimation obtained in presence of noise by applying TR and MUSIC to narrowband signals at f = fp, assuming for both signals an SNR of 10 dB and an additional path loss of 10 dB over a 50 MHz frequency band centered around fp.

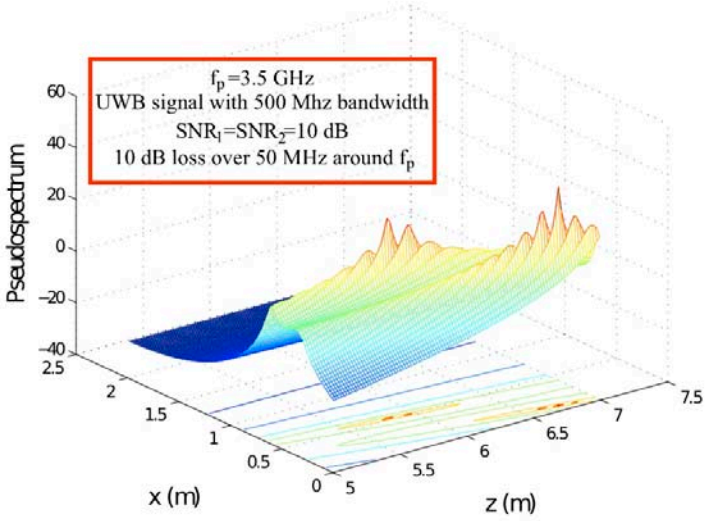

Figure 4-13: DOA estimation obtained in presence of noise by applying TR and MUSIC to UWB signals with a bandwidth W=500 MHz centered at f = fp, assuming for both signals an SNR of 10 dB and an additional path loss of 10 dB over a 50 MHz frequency band centered around fp.

5. Conclusion

In this deliverable, the most relevant models of coexistence of cognitive radio systems and legitimate systems are introduced. Decision parameters and the influence of the execution algorithm on the physical layer are described, including the constraints and requirements formulated by the decision engine, which define the interface between decision and execution. Parameters in the network/MAC layer and how they are mapped to physical layer are described, also are the parameters in the physical layer and how they are mapped to the hardware. Several signal processing and resource allocation algorithms are explained. Small-scale link-level and simplified system level assessments are used to compare performance of algorithms. Complexity assessment and feedback/control requirements are characterised.

Glossary and Definitions

Acronym	Meaning
ACF	Auto Correlation Function
ARQ	Automatic repeat request
AWGN	Additive White Gaussian Noise
CIR	Channel Impulse Response
CR	Cognitive Radios
CRN	Cognitive Radio Networks
CR	Cognitive Radio
CSI	Channel state information
DCPC	Distributed Constrained Power Control
DME	Distance Measuring Equipment
DOA	Direction Of Arrival
DPC	Dirty Paper Coding
DS	Direct Sequence
DTV	Digital Television
ECC	Electronic Communications Committee
EGC	Equal Gain Combining
EIRP	Equivalent Isotropically Radiated Power
FCC	Federal Communications Commission
FFT	Fast Fourier Transform
GDPC	Generalized Distributed Power Control
GPS	Global Positioning System
HOS	Higher Order Statistics
IFFT	Inverse Fast Fourier Transform
ITL	Interference Limit
IQ	In-phase Quadrature
LDPC	Low-density parity-check
MAC	Medium Access Control
MUI	Multi User Interference
MUSIC	MUltiple SIgnal Classification
OFDM	Orthogonal Frequency Division Multiplexing
OSI	Open Systems Interconnection
PAM	Pulse Amplitude Modulation
PPM	Pulse Position Modulation
PU	Primary User
SU	Secondary User

QoS	Quality of Service
RSSI	Received Signal Strength Indicator
SINR	Signal-to-Interference-Noise ratio
SNR	Signal to Noise Ratio
SU	Secondary User
TH-IR	Time Hopping Impulse Radio
TPC	Transmit Power Control
TOA	Time Of Arrival
TR	Time Reversal
UWB	Ultra Wide Band

6. References

[1] "Spectrum sensing," ACROPOLIS Deliverable 9.1, Sep. 2011.

[2] A. Ghasemi, et al., "Opportunistic Spectrum Access in Fading Channels through Collaborative Sensing," IEEE Journal of Communications, vol. 2, no. 2, pp. 71-81, March 2007.

[3] P. D. Sutton, et al., "Cyclostationary Signatures for Rendezvous in OFDM-Based Dynamic Spectrum Access Networks," 2nd IEEE International Symposium on New Frontiers in Dynamic Spectrum Access Networks, DySPAN 2007, June 2007.

[4] Federal Communications Commision, Tech. Rep. 08-260, Nov. 2008. Available: hraunfoss.fcc.gov/edocs public/attachmatch/FCC-08-260A1.pdf

[5] "Memorandam Opinion and Order on Reconstruction of the Seventh Report and Order and Eighth report and Order," Federal Communications Commision, Tech. Rep. 08-72, Mar. 2008. Available: hraunfoss.fcc.gov/edocs_public/attachmatch/FCC-08-72A1.pdf

[6] "List of All Class A, LPTV, and TV Translator Stations," Federal Communications Commission, Tech. Rep., 2008. Available: www.dtv.gov/MasterLowPowerList.xls

[7] "Report C from CEPT to the European Commission in response to the mandate on Technical considerations regarding harmonisation options for the digital dividend," CEPT-ECC, Tech. Rep., Jun 2008.

[8] A. Goldsmith, S. Jafar, I. Maric, and S. Srinivasa, "Breaking spectrum gridlock with cognitive radios: An information theoretic perspective," Proc. IEEE, vol. 97, no. 5, pp. 894-914, May 2009.

[9] S. Haykin, "Cognitive radio: brain-empowered wireless communications," IEEE J. Sel. Areas in Commun., vol. 23, no. 2, pp. 201-220, Feb. 2005.

[10] G. Scutari, D. Palomar, J.-S. Pang, and F. Facchinei, "Flexible design of cognitive radio wireless systems," IEEE Signal Process. Mag., vol. 26, no. 5, pp. 107-123, Sep. 2009.

[11] R. Zhang and Y.-C. Liang, "Exploiting multi-antennas for opportunistic spectrum sharing in cognitive radio networks," IEEE J. Sel. Topics in Signal Process., vol. 2, no. 1, pp. 88-102, Feb. 2008.

[12] R. Zhang and S. Cui, "Cooperative interference management with MISO beamforming," IEEE Trans. on Signal Processing, vol. 58, no. 10, pp. 5450-5458, Oct. 2010.

[13] R. Zhang, Y.-C. Liang, and S. Cui, "Dynamic resource allocation in cognitive radio networks," IEEE Signal Process. Mag., vol. 27, no. 3, pp. 102-114, May 2010.

[14] J. Lv and E. A. Jorswieck, "Spatial shaping in cognitive system with coded legacy transmission," in Proc. of International ITG Workshop on Smart Antennas (WSA), Feb. 2011.

[15] J. R. Hoffman, M. G. Cotton, R. J. Achatz, R. N. Statz, and R. A. Dalkejnm, "Measurements to Determine Potential Interference to GPS Receivers from Ultrawideband Transmission Systems," NTIA Report TR-01-384, February 2001.

[16] M. Hamalainen, V. Hovinen, R. Tesi, J. H. J. Iinatti, and M. Latva-aho, “On the UWB system coexistence with GSM900, UMTS/WCDMA, and GPS,” IEEE Journal on Selected Areas in Communications, vol. 20, no. 9, pp. 1712-1721, September 2002.

[17] M. G. Di Benedetto and G. Giancola, “Understanding Ultra Wide Band Radio Fundamentals,” Prentice Hall, 2004.

[18] Y. Wang, X. Dong, and I. J. Fair, “Spectrum Shaping and NBI Suppression in UWB Communications,” IEEE Transactions on Wireless Communications, vol. 6, no. 5, pp. 1944-1952, May 2007.

[19] J. A. Ney da Silva and M. L. R. de Campos, “Spectrally Efficient UWB Pulse Shaping With Application in Orthogonal PSM,” IEEE Transactions on Communications, vol. 55, no. 2, pp. 313-322, February 2007.

[20] M. Abtahi, J. Magne, M. Mirshafiei, L.A. Rusch, and S. LaRochelle, “Generation of Power-Efficient FCC-Compliant UWB Waveforms Using FBGs: Analysis and Experiment,” Journal of Lightwave Technology, vo. 26, no.5, pp. 628-635, March 2008.

[21] M.-G. Di Benedetto and L. De Nardis, “Tuning UWB Signals by Pulse Shaping: Towards context-aware wireless networks,” Special Issue on Signal Processing in UWB Communications, Signal processing, Elsevier Publishers, vo. 86, no. 9, pp. 2172-2184, September 2006.

[22] M. Biagi and V. Polli, “Ultra Wide Band Cognitive Pulse Shaping under Physical-Layer QoS Constraints,” IEEE Transactions on Communications, vol. 59, no. 11, pp. 3167-3176, November 2011.

[23] S. Gambini, L. De Nardis, E. Alon, and J. Rabaey “Interference robust self-mixing UWB systems using phase-domain spreading,” IEEE International Conference on UWB 2011 (ICUWB2011), Bologna, Italy, September 2011.

[24] D. Leenaerts, R. van de Beek, J. Bergervoet, H. Kundur, and G. van der Weide, “WiMedia UWB technology: 480Mb/s wireless USB,” IEEE International Workshop on Radio-Frequency Integration Technology (RFIT), 2007.

[25] B. Fa, F.-J. Han, A.-M. Zhang, and F.-J. Han, “Spectrum sensing in MB-OFDM based cognitive UWB systems coexistence with WiMax,” 11th IEEE Singapore International Conference on Communication Systems (ICCS), pp. 203-207, Nov. 2008.

[26] L. Feng, B. Li, W.-X. Zou, Z. Zhou, and X.-J. Huang, “Interference analysis for UWB coexistence with 3.5GHz WiMAX system,” International Symposium on Communications and Information Technologies (ISCIT), Oct. 2010.

[27] M. Li, D.-Q. Wang, Y.-X. Song, and Y.-Y. Yang, “Cognitive radio-based interference avoidance schemes for MB-OFDM UWB,” IEEE International Conference on Information Theory and Information Security (ICITIS), Dec. 2010.

[28] N. Devroye, P. Mitran, and V. Tarokh, “Achievable rates in cognitive radio channels,” IEEE Trans. on Information Theory, vol. 52, no. 5, pp. 1813-1827, May 2006.

[29] W. Wu, S. Vishwanath, and A. Arapostathis, “Capacity of a class of cognitive radio channels: Interference channels with degraded message sets,” IEEE Trans. on Information Theory, vol. 53, no. 11, pp. 4391-4399, Nov. 2007.

[30] A. Jovicic and P. Viswanath, “Cognitive radio: An information-theoretic perspective,” IEEE Trans. on Information Theory, vol. 55, no. 9, pp. 3945-3958, Sept. 2009.

[31] I. Maric, R. Yates, and G. Kramer, “Capacity of interference channels with partial transmitter cooperation,” IEEE Trans. on Information Theory, vol. 53, no. 10, pp. 3536-3548, Oct. 2007.

[32] E. Hossain, L. Le, N. Devroye, and M. Vu, ”Cognitive Radio: From Theory to Practical Network Engineering” in New Directions in Wireless Communications Research. Springer, 2009, ch. 10, pp. 251-289.

[33] M. Costa, "Writing on dirty paper". IEEE Trans. Inf. Theory, vol. 29, no. 3, pp. 439-441, May 1983.

[34] N. Michelusi, O. Simeone, M. Levorato, P. Popovski, and M. Zorzi, “Optimal cognitive transmission exploiting redundancy in primary ARQ process,” in Proc. Workshop on Inf. Theory and Applications (ITA).

[35] R. A. Tannious and A. Nosratinia, “Cognitive radio protocols based on exploiting hybrid ARQ retransmissions,” IEEE Transactions on Wireless Communications, vol. 9, no. 9, Sept. 2012.

[36] Y. Han, A. Pandharipande, and S. Ting, “Cooperative decode-and-forward relaying for secondary spectrum access,” IEEE Transactions on Wireless Communications, vol. 8, no. 10, pp. 4945–4950, Oct. 2009.

[37] Y. Li, P. Wang, and D. Niyato, “Optimal power allocation for secondary users in cognitive relay networks,” in Proc. IEEE Wireless Communications and Networking Conf. (WCNC), Mar. 2011, pp. 862–867.

[38] ACROPOLIS Deliverable 12.1 “Specification of Preliminary Set of Appropriate Metrics, Utility Functions and Layer Identification,” Sept. 2011.

[39] S. Mangold, S. Choi, G. R. Hiertz, O. Klein, and B. Walke, “Analysis of IEEE 802.11e for QoS support in wireless LANs,” IEEE Wireless Communications Magazine, vol. 10, no. 6, pp. 40-50, 2003.

[40] E. Jorswieck, R. Mochaourab, and M. Mittelbach, “Effective Capacity Maximization in Multi-Antenna Channels with Covariance Feedback,” IEEE Trans. on Wireless Communications, vol. 9, no. 10, pp. 2988-2993, Oct. 2010.

[41] I. Krikidis, N. Devroye, and J. S. Thompson, “Stability Analysis for Cognitive Radio with Multi-Access Primary Transmission,” IEEE Trans. on Wireless Communications, vol. 9, no. 1, Jan. 2010.

[42] F. P. Kelly, “Stochastic Networks: Theory and Applications,” Oxford University Press, ch. Notes on effective bandwidths, pp. 141-168, 1996.

[43] C.-S. Chang and J. A. Thomas, “Effective bandwidth in high-speed digital networks,” IEEE J. Sel. Areas Commun., vol. 13, pp. 1091-1100, Aug. 1995.

[44] D. Wu and R. Negi, “Effective capacity: a wireless link model for support of quality of service,” IEEE Trans. Wireless Commun., vol. 2, pp. 630-643, 2003.

[45] J. Tang and X. Zhang, “Quality-of-service driven power and rate adaptation over wireless links,” IEEE Trans. Wireless Commun., vol. 6, pp. 3058-3068, Aug. 2007.

[46] E. Biglieri, J. Proakis, and S. Shamai, “Fading channels: information theoretic and communications aspects,” IEEE Trans. Inf. Theory, vol. 44, pp. 2619-2692, 1998.

[47] D. Tse and P. Viswanath, “Fundamentals of Wireless Communication,” Cambridge University Press, Cambridge, UK, 2005.

[48] F. Halsall, “Data Communications, Computer Networks and Open Systems, Electronic Systems Engineering,” Addison-Wesley, Reading, Mass, USA, 4th edition, 1996.

[49] L. Yang and M.-S. Alouini, “Performance analysis of multiuser selection diversity,” IEEE Transactions on Vehicular Technology, vol. 55, no. 6, pp. 1848–1861, 2006.

[50] S. S. Kulkarni and C. Rosenberg, “Opportunistic scheduling policies for wireless systems with short term fairness constraints,” in Proceedings of IEEE Global Telecommunications Conference (GLOBECOM), San Francisco, California, USA, December 2003.

[51] R. Jain, D. Chiu, and W. Hawe, “A quantitative measure of fairness and discrimination for resource allocation in shared computer systems,” Research Report TR-301, DEC, New York, NY, USA, September 1984.

[52] R. Elliott, “A measure of fairness of service for scheduling algorithms in multiuser systems,” in Proceedings of the Canadian Conference on Electrical and Computer Engineering (CCECE), vol. 3, pp. 1583-1588, Winnipeg, Canada, May 2002.

[53] M. Sharif and B. Hassibi, “Delay considerations for opportunistic scheduling in broadcast fading channels,” IEEE Transactions on Wireless Communications, vol. 6, no. 9, pp. 3353-3363, 2007.

[54] R. A. Tannious and A. Nosratinia, “Cognitive radio protocols based on exploiting hybrid ARQ retransmissions,” IEEE Transactions on Wireless Communications, vol. 9, no. 9, Sept. 2012.

[55] Y. Han, A. Pandharipande, and S. Ting, “Cooperative decode-and-forward relaying for secondary spectrum access,” IEEE Transactions on Wireless Communications, vol. 8, no. 10, pp. 4945-4950, Oct. 2009.

[56] B. Zhao and M. C. Valenti, “Distributed Turbo coded diversity for relay channel,” Electron. Lett., vol. 39, no. 10, pp. 786-787, May 2003.

[57] Z. Zhang and T. M. Duman, “Capacity-approaching turbo coding and iterative decoding for relay channels,” IEEE Trans. on Comm., vol. 53, no. 11, pp. 1895-1905, Nov. 2005.

[58] Z. Si, R. Thobaben, and M. Skoglund, “A practical approach to adaptive coding for the three- node relay channel,” in Proc. IEEE Wireless Communications and Networking Conference (WCNC), Sydney, Australia, April 2010.

[59] A. Chakrabarti, A. de Baynast, A. Sabharwal, and B. Aazhang, “Low density parity check codes for the relay channel,” IEEE Journal on Sel. Areas in Comm., vol. 25, no. 2, pp. 1-12, Feb. 2007.

[60] P. Razaghi and W. Yu, “Bilayer low-density parity-check codes for decode-and-forward in relay channels,” IEEE Trans. on Inf. Theory, vol. 53, no. 10, pp. 3723-3739, Oct. 2007.

[61] Z. Si, R. Thobaben, and M. Skoglund, “Bilayer LDPC Convolutional Codes for Half-Duplex Relay Channels,” in Proc. IEEE International Symposium on Information Theory (ISIT), St. Petersburg, Russia, August 2011.

[62] J. Hagenauer, "Rate-compatible punctured convolutional codes (RCPC codes) and their applications," IEEE Transactions on Communications, vol. 36, no. 4, pp. 389-400, April 1988.

[63] Z. Si, M. Andersson, R. Thobaben, and M. Skoglund, “Rate-compatible LDPC convolutional codes for capacity-approaching hybrid ARQ,” in Proc. IEEE Information Theory Workshop (ITW), Oct. 2011.

[64] J. W. Byers, M. Luby, and M. Mitzenmacher, "A digital fountain approach to asynchronous reliable multicast," IEEE Journal on Selected Areas in Communications, vol. 20, no. 8, pp. 1528-1540, Oct. 2002.

[65] K. Azarian, H. El Gamal, and P. Schniter, “On the achievable diversity-multiplexing tradeoff in half-duplex cooperative channels,” IEEE Transactions on Information Theory, vol. 51, no. 12, pp. 4152-4172, Dec. 2005.

[66] Z. Si, R. Thobaben, and M. Skoglund, “Dynamic Decode-and-Forward Relaying with Rate-Compatible LDPC Convolutional Codes,” in Proc. International Symposium on Communications, Control and Signal Processing (ISCCSP), Rome, Italy, May 2012.

[67] B. Rimoldi and R. Urbanke, “A rate splitting approach to the Gaussian Multiple Access Channel”, IEEE Trans. Inf. Theory, vol. 42, no. 2, March 1996.

[68] W. Zhang and U. Mitra, “Spectrum shaping: a new perspective on cognitive radio-part I: coexistence with coded legacy transmission,” IEEE Trans. on Communications, vol. 58, no. 6, pp. 1857-1867, June 2010.

[69] W. Zhang and U. Mitra, “Spectrum shaping: a new perspective on cognitive radio-part II: coexistence with uncoded legacy transmission,” IEEE Trans. on Communications, vol. 58, no. 10, pp. 2971-2983, Oct. 2010.

[70] H. Weingarten, Y. Steinberg, and S. Shamai, “The Capacity Region of the Gaussian Multiple-Input Multiple-Output Broadcast Channel”, IEEE Transactions on Information Theory, vol. 52 no. 9, pp. 3936-3964, 2006.

[71] “Context Representation for Cognitive Radios and Networks,” ACROPOLIS Deliverable D8.1, Sept. 2011.

[72] M. Sternad, T. Svensson, and G. Klang, “The WINNER B3G system MAC concept,” in Proceedings of the IEEE Vehicular Technology Conference, pp. 3037-3041, 2006.

[73] E. Jorswieck, A. Sezgin, B. Ottersten, and A. Paulraj, "Feedback Reduction in Uplink MIMO OFDM Systems by Chunk Optimization", Special Issue on MIMO Transmission with Limited Feedback, EURASIP Journal on Advances in Signal Processing, 2008.

[74] J. Lv, R. B. Serrano, E. A. Jorswieck, R. Thobaben, and A. Kliks, “Optimal beamforming in MISO cognitive channels with degraded message sets,” IEEE Wireless Communications and Networking Conference (WCNC 2012), accepted.

[75] G. Caire and S. Shamai (Shitz), “On the achievable throughput of a multiantenna Gaussian broadcast channel,” IEEE Trans. on Information Theory, vol. 49, no. 7, pp. 1691-1706, Jul. 2003.

[76] “Digital Dividend: Cognitive Access, Consultation on Licence-Exempting Cognitive Devices using Interleaved Spectrum,” OFCOM, February 2009.

[77] J. Zander. “Performance of optimum transmitter power control in cellular radio systems,” IEEE Trans. Vehicular Technology, vol. 41, no. 1, pp. 57-62, Feb. 1992.

[78] G. J. Foschini and Z. Miljanic, “A simple distributed autonomous power control algorithm and its convergence,” IEEE Trans. Veh. Tech., vol. 42, pp. 641-646, Apr. 1993.

[79] S. Grandhi, J. Zander, and R. Yates, “Constrained power control,” Int. J. Wireless Personal Commun., vol. 1, no. 4, Apr. 1995.

[80] F. Berggren, R. Jäntti, and S.-L. Kim, “A general algorithm for constrained power control with capability of temporal removal,” IEEE Transactions on Vehicular Technology, vol. 50, no. 6, pp. 1604-1612, 2001.

[81] L. Zhang, Y.-C. Liang, and Y. Xin, “Joint Admission Control and Power Allocation for Cognitive Radio Networks,” IEEE ICASSP 2007.

[82] D. Niyato and E. Hossain, “A Game-Theoretic Approach to Competitive Spectrum Sharing in Cognitive Radio Networks,” IEEE WCNC 2007.

[83] N. Hoven and A. Sahai, “Power scaling for cognitive radio,” International Conference on Wireless Networks, Communications and Mobile Computing, June 2005.

[84] K. Hamdi, Wei Zhang, and K. Ben Letaief, “Power Control in Cognitive Radio Systems Based on Spectrum Sensing Side Information,” IEEE International Conference on Communications, June 2007.

[85] Y.-J. Yu, H. Murata, K. Yamamoto, and S. Yoshida, “Multi-Hop Cooperative Sensing and Transmit Power Control based on Interference Information for Cognitive Radio,” IEEE 18th International Symposium on Personal, Indoor and Mobile Radio Communications, Dec. 2007.

[86] L. Qian, X. Li, J. Attia, and Z. Gajic, “Power Control for Cognitive Radio Ad Hoc Networks,” 15th IEEE Workshop on Local & Metropolitan Area Networks, June 2007.

[87] S. Im, H. Jeon, and H. Lee, “Autonomous Distributed Power Control for Cognitive Radio Networks,” IEEE Vehicular Technology Conference, Sept. 2008.

[88] F. F. Digham, M. S. Alouini, and M. K. Simon, “On the Energy Detection of Unknown Signals Over Fading Channels,” IEEE Transactions on Communications, vol. 55, no. 1, pp. 21-24, Jan. 2007.

[89] K. Arshad and K. Moessner, “Collaborative spectrum sensing for cognitive radio,” Joint Workshop on Cognitive Wireless Networks andSystems, 2009.

[90] C. E. Perkins and E. M. Royer, “Ad hoc on-demand distance vector routing,” IEEE WMCSA, February 1999.

[91] M. Fink, “Time-reversal waves and super resolution,” Journal of Physics: Conference Series 124 (2008), 4th AIP International Conference and the 1st Congress of the IPIA.

[92] A. Derode, P. Roux, and M. Fink, “Robust acoustic time reversal with high-order multiple scattering,” Phys. Rev. Letters, vol. 75, pp. 4206-4209, 1995.

[93] E. A. Abiodun, R. C. Qiu, and N. Guo, “Demonstrating Time Reversal in Ultra-wideband Communications Using Time Domain Measure- ments,” 51st International Instrumentation Symposium, May 2005.

[94] S. Xiao, J. Chen, X. Liu, and B.-Z. Wang, “Spatial focusing characteristics of time reversal UWB pulse transmission with different antenna arrays,” Progress In Electromagnetics Research B, vol.2, pp. 223-232, 2008.

[95] L. De Nardis, J. Fiorina, D. Panaitopol, and M.-G. Di Benedetto, “Combining UWB with Time Reversal for improved communication and positioning,” Springer Telecommunication Systems, 2011.

[96] J. Fiorina and D. Domenicali, “The non validity of the gaussian approximation for multi-user interference in ultra wide band impulse radio: from an inconvenience to an advantage,” IEEE Transactions on Wireless Communications, vol. 8, no. 11, pp. 5483-5489, November 2009.

[97] R. O. Schmidt, “Multiple Emitter Location and Signal Parameter Estimation,” IEEE Transactions on antennas and propagation, vol. 34, no. 3, pp. 276-280, March 1986.

[98] L. Borcea, G. C. Papanicolaou, C. Tsogka, and J. Berryman, “Imaging and time reversal in random media,” Inverse Problems, vol. 18, no. 5, pp. 1247-1279, 2002.